AFCRL 63-429

THE KINETIC-ENERGY BUDGET OF THE STRATOSPHERE OVER NORTH AMERICA DURING THE WARMING OF 1957

by
M. A. LATEEF
Department of Meteorology
Florida State University

Contract No. AF 19(628)-394
Project No. 8604
Task No. 860405

SCIENTIFIC REPORT NO. 1
15 April 1963

PREPARED FOR

AIR FORCE CAMBRIDGE RESEARCH LABORATORIES
OFFICE OF AEROSPACE RESEARCH
UNITED STATES AIR FORCE
BEDFORD, MASSACHUSETTS

AFCRL 63-429

THE KINETIC-ENERGY BUDGET OF THE STRATOSPHERE OVER NORTH AMERICA DURING THE WARMING OF 1957

by

M. A. LATEEF

Department of Meteorology

Florida State University

Contract No. AF 19(628)-394

Project No. 8604

Task No. 860405

SCIENTIFIC REPORT NO. 1

15 April 1963

Prepared for

Air Force Cambridge Research Laboratories
Office of Aerospace Research
United States Air Force
Bedford, Massachusetts

Requests for additional copies by Agencies of the Department of Defense, their contractors, and other Government agencies should be directed to the:

ARMED SERVICES TECHNICAL INFORMATION AGENCY
ARLINGTON HALL STATION
ARLINGTON 12, VIRGINIA

Department of Defense contractors must be established for ASTIA services or have their "need-to-know" certified by the cognizant military agency of their project or contract.

All other persons and organizations should apply to the:

U. S. DEPARTMENT OF COMMERCE
OFFICE OF TECHNICAL SERVICES
WASHINGTON 25, D. C.

ACKNOWLEDGMENTS

The author is grateful to Professor Richard A. Craig for his guidance throughout the course of this investigation. Thanks are extended to Messrs. W. J. Koss, R. S. Hawkins and P. R. Sticksel for aid and cooperation during the programming of the IBM 709 computer. A portion of the programming costs of this investigation was borne by the National Science Foundation.

Appreciation is also due to Professor R. J. Reed of the University of Washington for communicating to the author results of some of his computations.

TABLE OF CONTENTS

LIST OF TABLES

LIST OF ILLUSTRATIONS

ABSTRACT

The large and rapid decrease in kinetic energy of the lower stratosphere (100-25 mb) during the warming of mid-January to mid-February, 1957, has been investigated in terms of energy transport and generation processes. These processes are represented by the corresponding terms in the mechanical energy equation.

The evaluation of these terms was carried out using the 100-mb, 50-mb and 25-mb values of geopotential, temperature, the geostrophic wind components and adiabatic vertical motion at each point of a grid covering most of the North American continent and the adjacent North Atlantic. The investigation considered a limited volume which exchanged energy with the surrounding atmosphere through the vertical boundaries as well as through the upper and lower boundary pressure surfaces.

Terms in the kinetic energy budget explicitly involving existing kinetic energy were found to be negligible in comparison with the other terms. Conversion of energy within the volume was from kinetic to potential energy throughout most of the period.

Kinetic energy was generated through vertical motions at the upper boundary pressure surface and dissipated through vertical motions at the lower boundary pressure surface. The net effect was a gain in kinetic energy during the early part of the warming period and a loss of kinetic energy during the latter part. The contributions to kinetic energy changes on layers of limited depth due to generation of kinetic

energy at the upper and lower boundaries can be quite significant.

During the early stages of the warming, the volume lost kinetic energy by dissipation through horizontal motions at the vertical boundaries. But during the period of pronounced warming throughout the volume, a large gain in kinetic energy was brought about by generation at the vertical boundaries. This generation process acted as a major source of kinetic energy for the volume and hence a major sink of kinetic energy for the lower stratosphere at other longitudes.

For the volume and time period chosen for study, large scale sinking motion at the pressure surfaces accounted for almost all of the energy transformation and vertical flux processes.

The values of the horizontal and vertical fluxes of energy and of the total conversion rates were balanced against the local change in kinetic energy of the volume. The residual was taken as an approximation to the rate of dissipation of kinetic energy by small scale motions. These rates appear reasonable when compared with those of the other processes in the volume.

1. INTRODUCTION

In recent years, as a result of increased frequency of observations reaching above 20 km, several studies have been made of stratospheric circulation and in particular of the warming phenomena during the winter months. Scherhag (1952) first reported a warming at stratospheric levels based on ascents over Berlin. Since then, other reports of such warming during successive winters have prompted the acceptance of large temperature fluctuations as a characteristic of wintertime stratospheric circulation. The evolution of the warming as regards the location and intensity has varied from year to year. But the basic feature has involved a fundamental change in the stratospheric general circulation from the early winter type, consisting of a cold circumpolar cyclonic vortex, to the spring-summer type with light winds around a warm polar anticyclone.

The stratospheric warming in the winter of 1956-1957 was of particular significance not only because of the rapidity with which temperatures rose at levels above 100 mb but also from the point of view of its location over North America. The initial stages of the warming (at least at and below the 25 mb level) took place over southeastern Canada and the subsequent passage of the warm center occurred over an area of relatively good data coverage, according to stratospheric standards. The evolution of the temperature and wind fields during this warming has been described by Teweles (1958) and by Craig and Hering (1959). Although such descriptions are of importance, an

investigation of changes in the vertical motion patterns and associated energy transformations would be of great use in adding to our knowledge of the dynamics of such warmings.

Basic analyses of the height and temperature fields at 100 mb, 50 mb and 25 mb during the period 16 January to 15 February, 1957 have been carried out by the stratospheric circulation research group at the Florida State University. The period chosen includes a week or so prior to any obvious evidence of warming at 25 mb and below, and also extends to a few days after the most marked temperature changes had occurred. The analysis area is shown in Fig. 1. Both the size of the analysis area and the upper limit to the pressure surface were dictated by data considerations. Values of various parameters at the three pressure levels over a grid of 132 points have been made available on punched cards. These include values of the geopotential height, temperature, the geostrophic wind components and vertical motion as computed from the adiabatic form of the first law of thermodynamics. Many of the details of the methods of analysis and computations of vertical motion and vorticity values have been described in published reports (Craig, Lateef and Mitchem, 1961a, 1961b; Craig and Lateef, 1961). A summary of the vertical motions has also been presented by Craig and Lateef (1962).

Studies of energy conversions at stratospheric levels have been restricted in the past owing to scarcity of data on vertical motions at these levels. Recent attempts to evaluate kinetic energy generation and dissipation processes in the lower stratosphere were generally confined to levels at and below 50 mb. A brief summary of previous

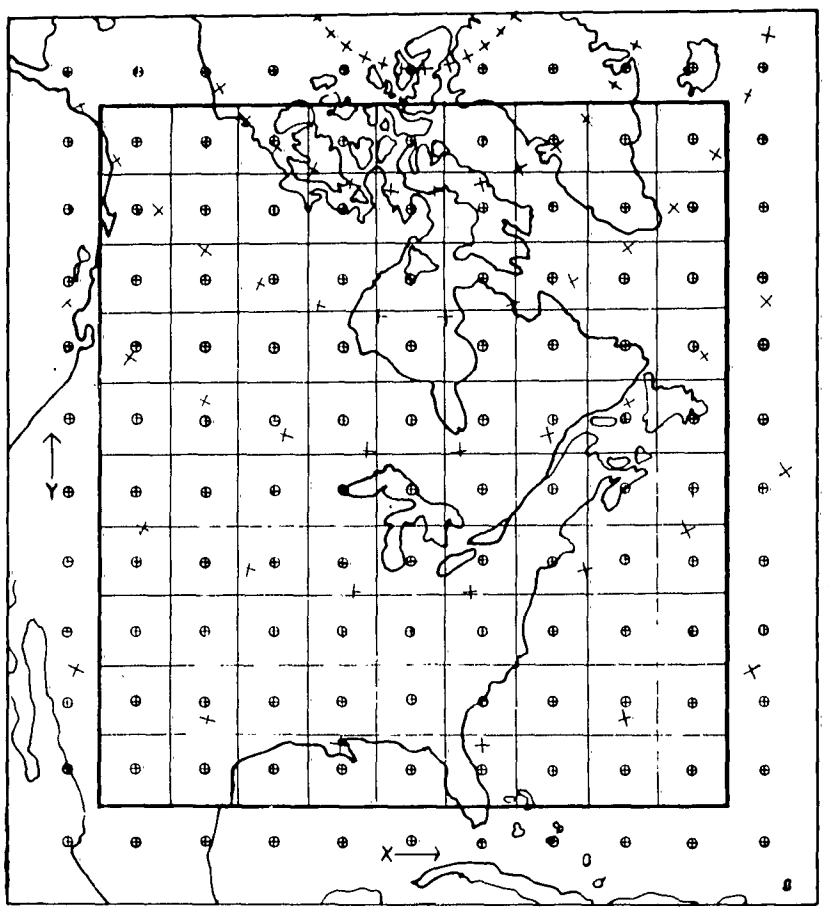

Fig. 1. Base map used for analyses and grid points at which computations have been made. The crosses indicate intersections of latitude and longitude at 10 degree intervals, the circled crosses indicate grid points. The perimeter of the grid is shown in heavy lines.

studies on the maintenance of kinetic energy of stratospheric motions is given in Section 3 of this report.

Although the analysis area covered only a small portion of the Northern Hemisphere, it was felt that the availability of data especially on vertical motions up to 25 mb and over a sufficiently dense grid justified an investigation of the magnitudes of the terms that enter into the kinetic energy budget. The computed values of the various terms would indicate the relative importance of the physical processes contributing to the kinetic energy changes of the volume under study. The details of the computational procedures are given in Section 4.

In order to make the results of the computations more understandable, a brief resume of the warming in terms of the evolution of the height and temperature fields and of the vertical motion patterns is presented in Section 5.

The rest of the report is devoted to discussion of the results of the computations. The time variation of horizontal kinetic energy in the volume bounded by the perimeter of the grid and the 100-mb and 25-mb pressure surfaces is presented in Section 6. The magnitudes of the various processes which bring about the change in kinetic energy are given in the later sections.

In contrast to previous investigations of kinetic energy on a hemispheric basis, this investigation considered a limited volume which exchanged energy with the surrounding atmosphere through its vertical boundaries as well as through the upper and lower pressure surfaces. Specific results concerning both the horizontal and vertical energy

transfers through the boundaries are treated in Sections 7 and 8, while the magnitudes of the conversion processes between kinetic and potential energy are discussed in Section 9.

The limited longitudinal extent of the volume did not allow evaluation of the energy transfer and conversion processes in terms of motions on a hemispheric scale. Analyses of the processes in the volume on the basis of mean motion and departures from the mean, averaged both over the area and over suitable time intervals during the period, was, however, undertaken. The results revealed by such analyses are included in Section 10. For the sake of completeness in the kinetic energy budget of the volume, estimates of the rate of frictional dissipation of kinetic energy within the volume were made as described in Section 11.

2. THE MECHANICAL ENERGY EQUATION

Since on a synoptic scale, vertical motion is much smaller in magnitude than horizontal motion, kinetic energy of horizontal motion can be considered equivalent to the total kinetic energy. The mathematical expression that represents the balance equation for horizontal kinetic energy can be derived from the scalar product of the horizontal wind and the equation of motion.

Derivation

Using the x, y, p, t-coordinate system, the horizontal equations of motion may be written

$$\frac{\partial u}{\partial t} + u\frac{\partial u}{\partial x} + v\frac{\partial u}{\partial y} + \omega\frac{\partial u}{\partial p} = -\frac{\partial \phi}{\partial x} + fv + F_x \qquad (1)$$

$$\frac{\partial v}{\partial t} + u\frac{\partial v}{\partial x} + v\frac{\partial v}{\partial y} + \omega\frac{\partial v}{\partial p} = -\frac{\partial \phi}{\partial y} - fu + F_y \qquad (2)$$

where u and v are the horizontal wind components in the x and y directions and $\omega = \frac{dp}{dt}$ is the individual pressure change representing vertical motion in this coordinate system where pressure replaces height as the vertical coordinate. ϕ is the geopotential of an isobaric surface, f is the Coriolis parameter, and F_x and F_y are the horizontal components of the frictional force per unit mass.

Multiplying equation (1) by u and equation (2) by v and adding them, leads to the following equation.

$$\frac{\partial k}{\partial t} + u\frac{\partial k}{\partial x} + v\frac{\partial k}{\partial y} + \omega\frac{\partial k}{\partial p} = -\left(u\frac{\partial \phi}{\partial x} + v\frac{\partial \phi}{\partial y}\right) + \left(u F_x + v F_y\right) \qquad (3)$$

where $k = \frac{u^2 + v^2}{2}$, is the horizontal kinetic energy per unit mass.

Equation (3) may be re-written as follows.

$$\frac{\partial k}{\partial t} + \frac{\partial}{\partial x}(ku) + \frac{\partial}{\partial y}(kv) + \frac{\partial}{\partial p}(k\omega) - k\left(\frac{\partial u}{\partial x} + \frac{\partial v}{\partial y}\right) - k\frac{\partial \omega}{\partial p} =$$

$$-\left(u\frac{\partial \phi}{\partial x} + v\frac{\partial \phi}{\partial y}\right) + \left(u F_x + v F_y\right) \qquad (4)$$

The last two terms on the left side of (4) cancel each other, since by the equation of continuity, $\frac{\partial u}{\partial x} + \frac{\partial v}{\partial y} + \frac{\partial \omega}{\partial p} = 0$.

We now select a volume bounded from the surrounding atmosphere by vertical boundaries extending from a constant pressure surface, p_0 to another pressure surface, p. Let A denote the area of intersection between the vertical boundaries and a constant isobaric surface, and L be the perimeter of this area. Both A and L are considered independent of height or pressure.

Integrating (4) over the volume specified above, or strictly speaking over the mass of the atmosphere between the two constant pressure surfaces and the vertical boundaries, leads to the following equations.

$$\int_p^{p_0}\int_A \frac{\partial k}{\partial t}\,dA\,\frac{dp}{g} + \int_p^{p_0}\int_A \left[\frac{\partial}{\partial x}(ku) + \frac{\partial}{\partial y}(kv)\right] dA\,\frac{dp}{g} + \int_p^{p_0}\int_A \frac{\partial}{\partial p}(k\omega)\,dA\,\frac{dp}{g} =$$

$$\int_p^{p_0}\int_A \left(u\frac{\partial \phi}{\partial x} + v\frac{\partial \phi}{\partial y}\right) dA\,\frac{dp}{g} - D \qquad (5)$$

where $$D = \int_{p}^{p_0} \int_{A} \left(u F_x + v F_y \right) dA \frac{dp}{g} \qquad (6)$$

is the rate at which horizontal kinetic energy of the portion of the atmosphere being considered, is changing owing to frictional dissipation forces.

If we now specify p_0 = 100 mb and p = 25 mb, we may consider the first term in (5), namely $\int_{p}^{p_0} \int_{A} \frac{\partial k}{\partial t} dA \frac{dp}{g}$, to be equivalent to $\frac{\partial}{\partial t} \int_{p}^{p_0} \int_{A} k dA \frac{dp}{g}$. Let K denote the expression $\int_{p}^{p_0} \int_{A} k dA \frac{dp}{g}$, which is the total kinetic energy of the mass of the portion of the atmosphere defined by A and the 100-mb and 25-mb pressure surfaces. Since p_0 and p have been assigned specific values, the mass of the atmosphere between these pressure levels and the vertical boundaries remains constant. The term $\partial K/\partial t$, therefore, actually represents the time variation of the total kinetic energy of this constant mass. Since we ordinarily use data at constant pressure levels instead of at fixed heights in the atmosphere, it has become customary to speak of "volume" in the x, y, p coordinate system corresponding to the geometric volume defined in the x, y, z system. Hence, the word "volume" wherever used in this report actually denotes the constant mass of the atmosphere between the specified pressure levels and the vertical boundaries.

From equation (5), on re-arranging terms, we get

$$\frac{\partial K}{\partial t} = -\frac{1}{g} \int_{p}^{p_0} \int_{A} \left[\frac{\partial}{\partial x} (ku) + \frac{\partial}{\partial y} (kv) \right] dAdp - \frac{1}{g} \int_{p}^{p_0} \int_{A} \frac{\partial}{\partial p} (k\omega) \, dAdp$$
$$- \frac{1}{g} \int_{p}^{p_0} \int_{A} \left(u \frac{\partial \phi}{\partial x} + v \frac{\partial \phi}{\partial y} \right) dAdp - D \qquad (7)$$

The first term on the right side of (7) is the divergence of a horizontal vector with components uk and vk. Therefore, applying a two dimensional form of the divergence theorem,

$$\int_A \left[\frac{\partial}{\partial x}(ku) + \frac{\partial}{\partial y}(kv)\right] dA = \oint_L kv_n \, dL \tag{8}$$

Equation (7) can be re-written:

$$\frac{\partial K}{\partial t} = -\frac{1}{g}\int_{p}^{p_0}\left(\oint_L kv_n \, dL\right)dp - \frac{1}{g}\int_{p}^{p_0}\frac{\partial}{\partial p}\left(\int_A k\omega dA\right)dp$$

$$-\frac{1}{g}\int_{p}^{p_0}\left(\int_A \underline{V}\cdot\nabla\phi \, dA\right)dp - D \tag{9}$$

where the new symbols have the following meanings:

v_n is horizontal wind component perpendicular to the vertical boundary of the volume, positive outward.

$\underline{V}$ is horizontal vector wind.

∇ is horizontal del operator along a constant pressure surface.

$$\text{The term } \underline{V}\cdot\nabla\phi = \nabla\cdot\phi\underline{V} - \phi\nabla\cdot\underline{V} \tag{10}$$

But, since $\nabla\cdot\underline{V} = -\frac{\partial\omega}{\partial p}$ and $\frac{\partial\phi}{\partial p} = -\alpha$, where $\alpha = \frac{1}{\rho}$ is the specific volume, we may write (10) as

$$\underline{V}\cdot\nabla\phi = \nabla\cdot\phi\underline{V} + \frac{\partial}{\partial p}(\phi\omega) + \omega\alpha \tag{11}$$

Substitution of (11) into equation (9) and use of the divergence theorem finally yields

$$\frac{\partial K}{\partial t} = -\frac{1}{g}\int_{p}^{p_o}\left(\oint_L kv_n\, dL\right) dp + \frac{1}{g}\left[\left(\int_A k\omega dA\right)_p - \left(\int_A k\omega dA\right)_{p_o}\right]$$

$$-\frac{1}{g}\int_{p}^{p_o}\left(\oint_L \phi v_n\, dL\right) dp + \frac{1}{g}\left[\left(\int_A \phi\omega\, dA\right)_p - \left(\int_A \phi\omega\, dA\right)_{p_o}\right]$$

$$-\frac{R}{g}\int_{p}^{p_o}\left(\int_A \frac{\omega T}{p}\, dA\right) dp - D \qquad (12)$$

where R is gas constant for dry air, T is temperature and the subscript p and p_o refer to the upper and lower boundary values of the corresponding terms.

Physical meaning of the terms

The term $\partial K/\partial t$ on the left side of equation (12) is the time-change of the total horizontal kinetic energy in the volume bounded by the perimeter L and the two specific pressure levels p_o and p.

The physical processes which bring about changes in K are represented by the terms on the right side of equation (12). Thus, the total horizontal kinetic energy may be changing as a result of:

(a) Advection of kinetic energy into the volume across the vertical boundary. This is represented by the term

$$(kv_n) = -\frac{1}{g}\int_{p}^{p_o}\left(\oint_L kv_n\, dL\right) dp$$

(b) Advection of kinetic energy into the volume through the boundary pressure surfaces. This is represented by the term

$$(k\omega) = \frac{1}{g}\left[\left(\left(\int_A k\omega \, dA\right)_p - \left(\int_A k\omega \, dA\right)_{p_0}\right]\right.$$

(c) Generation of kinetic energy through horizontal motions across the vertical boundary. This is represented by the term

$$(\phi v_n) = -\frac{1}{g}\int_p^{p_0}\left(\oint_L \phi v_n \, dL\right) dp$$

(d) Generation of kinetic energy through vertical motions at the boundary pressure surfaces. This is represented by the term

$$(\phi\omega) = \frac{1}{g}\left[\left(\int_A \phi\omega \, dA\right)_p - \left(\int_A \phi\omega \, dA\right)_{p_0}\right]$$

(e) Generation of kinetic energy within the volume by conversion from potential energy. This is represented by the term

$$(\omega T) = -\frac{R}{g}\int_p^{p_0}\left(\int_A \frac{\omega T}{p} \, dA\right) dp$$

(f) Generation of kinetic energy by motions of smaller scale than are included in the analysis. The effect of such motions on the kinetic energy of larger scales of motion would ordinarily amount to a dissipation of the latter, and is represented by the term D.

Because of their origin in the mathematical development of the $\underline{V} \cdot \nabla\phi$ term in equation (9), the (ϕv_n) and $(\phi\omega)$ terms form part of the total generation process, represented by the integral of $\underline{V} \cdot \nabla\phi$. Over the entire mass of the atmosphere, these two terms would vanish and the generation process would then be given by the integral of ωT, as shown

in equation (12). For the limited volume, however, the total generation process may be considered as the sum of processes depending on the boundary values of the variables, namely the (ϕv_n) and $(\phi\omega)$ processes and those involving values within the volume or the $(\omega\Gamma)$ process.

In the x, y, z, t system, it can be shown (Starr, 1948) that the generation process denoted by the integral of $\underline{V} \cdot \nabla p$ includes a $(p\ v_n)$ term representing the "performance of work by pressure forces at the boundary in virtue of displacements due to the horizontal velocity components." Inasmuch as ϕ and ω in the x, y, p, t system play roles similar to p and w in the x, y, z, t system, one can attribute similar modes of production of kinetic energy at the boundaries of the volume through the (ϕv_n) and $(\phi\omega)$ processes.

Under geostrophic equilibrium assumed for horizontal motions used in the evaluation of ω,

$$\omega = - g \rho w + \rho g \frac{\partial z}{\partial t} \tag{13}$$

where $w \left(= \frac{dz}{dt}\right)$ is the vertical velocity in the x, y, z system. Equation (13) indicates that the $(\phi\omega)$ term not only represents work done on air particles as they move vertically through the pressure surfaces but also involves release of kinetic energy through changes in potential energy of the atmospheric layer due to movement of the bottom or top surface of the mass being considered.

To the extent that the boundary generation processes are interlinked with the volume generation process $(\omega\Gamma)$, the (ϕv_n) and $(\phi\omega)$ processes are not pure boundary effects. They may, however, be viewed as adjustment processes in response to internal redistribution of mass

brought about by the (ωT) process in the volume. The specific nature of generation of kinetic energy by the (ϕv_n) and $(\phi\omega)$ terms as related to corresponding potential energy changes, is not so obvious. However, their inclusion in kinetic energy generation rates in limited atmospheric volumes would be necessary to obtain a better estimate of the total generation processes.

Previous applications

In many previous applications of equation (12), attention has been focused on computation of the (ωT) term. It is often possible to consider a volume that extends over the hemisphere. The (kv_n) and (ϕv_n) terms are then zero, if horizontal transports across the equator are neglected. If the volume is based at the earth's surface and extends high enough so that interaction with the overlying atmosphere may be neglected, then the $(k\omega)$ and $(\phi\omega)$ terms are zero.

Palmén (1960) has discussed applications of equation (12) to a volume extending from the surface of the earth to the top of the atmosphere but over a limited area. He has called $\underline{V} \cdot \nabla\phi$, appearing in equation (9), the "work" term, representing work done by the horizontal pressure forces inside the volume. For the volume used by Palmén, the (ϕv_n) and (ωT) terms acting together constitute the generation process.

Jensen (1960) has applied equation (12) over the Northern Hemisphere but between the surface and 50-mb pressure level. According to him, the $(\phi\omega)$ and (ωT) terms together constitute the transformation process. The transformation process now denoted by

$$\frac{1}{g}\left[\left(\int_A \phi\omega \, dA\right)_p - \left(\int_A \phi\omega \, dA\right)_{p_0}\right] - \frac{R}{g}\int_p^{p_0}\left(\int_A \frac{\omega T}{p} \, dA\right) dp,$$

involves not only the familiar correlation between ω and T but also the boundary value of the net correlation between ω and ϕ.

The dissipation term D is usually not computed directly, but obtained as a residual arising out of any imbalance among the other terms. In cases of computation of the conversion or transformation process denoted by (ωT) alone, the value of this term is often taken as an estimate of the dissipation rate of kinetic energy over a long period of time during which $\partial K/\partial t$ is assumed to be zero.

involves not only the familiar correlation between ω and T but also the boundary value of the net correlation between ω and ϕ.

The dissipation term D is usually not computed directly, but obtained as a residual arising out of any imbalance among the other terms. In cases of computation of the conversion or transformation process denoted by (ωT) alone, the value of this term is often taken as an estimate of the dissipation rate of kinetic energy over a long period of time during which $\partial K/\partial t$ is assumed to be zero.

3. PREVIOUS INVESTIGATIONS

Among previous investigations of the energy budget of the stratosphere, those of White and Nolan (1960), Wolfe (1960), Reed (1962), Jensen (1960) and Barnes (1962) are particularly relevant to the present study.

White and Nolan (1960) considered a volume limited in the horizontal by latitudes 30N and 60N and longitudes 70W and 120W and bounded by the 200-mb and 25-mb pressure surfaces. They studied the time period 28 January to 3 February, 1957. Average values of ω and α were obtained for the layers 200-50 mb and 100-25 mb. Considering these values to be representative of ω and α fields at the 100 and 50-mb levels, they computed the (ωT) term mentioned in Section 2, namely, the conversion of potential to kinetic energy within the volume. They found this term to be negative at 50 mb that is, to give conversion from kinetic to potential energy. The magnitude of the conversion process at 100 mb was nearly zero. Although they did not compute other terms in the kinetic energy balance equation, they concluded that the kinetic energy of the stratosphere is supplied by interaction with the adjacent layers above and below the volume through transport of existing kinetic energy.

Wolfe (1960) investigated the rate of change of kinetic energy of the horizontal wind and the conversion from potential to kinetic energy at the 50-mb level for the warming period 25 January to 9 February, 1957. His region comprised the latitude belt between 35N and 80N. Analysis was done for only 4 maps during the period. According to him,

the kinetic energy of the horizontal wind showed a rapid and large depletion due to a large scale decrease of kinetic energy of the zonal winds. The kinetic energy of the eddy flow showed a small, probably insignificant decrease during this same period. The total conversion of energy amounted to a conversion of potential to kinetic energy although the conversion from zonal potential to zonal kinetic energy was opposite in sign. This would contradict the results of White and Nolan (1960), for the same level, but for a shorter period and over a smaller region. An apparent discrepancy arose between the total rate of change of kinetic energy and the total rate of conversion of available potential energy to kinetic energy. This was explained as due to treating the 50-mb lamina as a closed system and neglecting vertical flux of energy through the lower boundary of the lamina.

Reed (1962) has extended the previous investigations and computed the changes in both the zonal and eddy components of kinetic and potential energies as well as corresponding conversion rates for the two periods 25 January to 4 February and 4 February to 9 February, 1957. He found a steady almost linear decline in the zonal kinetic energy during the entire period. But between 25 January and 4 February, while zonal kinetic energy decreased, eddy kinetic energy increased due to conversions to and from corresponding potential energy sources. After 4 February, however, these changes reversed their direction; a decrease in eddy kinetic energy occurred while there was an apparent increase in zonal kinetic energy contrary to the decrease actually observed. He pointed out that conversion processes alone could not account for this discrepancy. It appeared plausible that the loss of

zonal kinetic energy during the period 4 February to 9 February, "despite the indications that other forms of energy were being transformed into this form of energy, could be attributed to a net vertical outflow of geopotential through the base of the stratosphere."

Jensen (1960) carried out computations based on data for January 1958 for about 100 stations in the Northern Hemisphere between 20N and 80N in a belt including all longitudes. He considered the volume from the surface to 50 mb and neglected any interactions with the atmosphere above. With regard to results applicable to the stratosphere, he found that the generation term (ωT) was positive, although in some layers certain eddy processes into which this term can be subdivided, had the opposite sign. More specifically, he found that the stratospheric layer from 200 to 50 mb was characterized by an overall positive energy transformation from potential to kinetic energy although there was evidence of a reverse transformation in the top boundary layer from 100 to 50 mb. The ($\phi\omega$) term was evaluated on the assumption that this term was zero at the 50-mb surface. The contribution to the total kinetic energy generation rate in the 100-50 mb layer, due to this term was found to be positive. Neglecting any net transport in the vertical of kinetic energy across the stratospheric layers, dissipation rates were estimated as follows. It was first assumed that the change in kinetic energy during the analysis period was negligible. Accordingly, values corresponding to the ($\phi\omega$) and (ωT) terms were introduced into the balance equation (12), and the residual was taken to represent the dissipation rate.

Barnes (1962) utilized observations at 100, 50, 30 and 10-mb levels from 212 stations in the Northern Hemisphere for the period July

to December 1957. He found that in the lower stratosphere, defined by the layer 100 to 50 mb, adiabatic vertical motions resulted in an overall conversion from kinetic to potential energy, in agreement with the findings of Jensen (1960). But above 40 mb, the conversions seemed to be in the opposite sense.

The $(\phi\omega)$ term was found by Barnes to be one of the most important terms in the kinetic energy balance equation. Computations of this term indicated that generation of kinetic energy at the 75-mb and 40-mb levels acted to increase the kinetic energy of the layers above these levels. Values at 20 mb pointed to an increase in kinetic energy of the layer below. But according to him, these values at 20 mb were very suspect because of the small number of observations reaching 10 mb. Advection of existing kinetic energy was found to be inadequate to account for the large increase in kinetic energy from October through December 1957.

More detailed studies are needed to add to and supplement those already done for the stratospheric region. Further investigations utilizing data above 50 mb are required to confirm or modify the conclusions reached by previous investigators. While data on a hemispheric basis would certainly be most valuable and desirable, there are serious limitations on obtaining adequate observations reaching even 50 mb. The availability of data reaching 25 mb, during the stratospheric warming of 1957, although for a short period and over a limited volume, makes it possible to attempt a more detailed investigation of energy transformation and flux processes in the lower stratosphere. The details of the computational procedure used in the evaluation of all the

terms in the mechanical energy equation (12) are presented in the next section.

4. COMPUTATIONAL PROCEDURES

The roles of the various physical processes which affect the balance of kinetic energy in a limited atmospheric volume are expressed by the various terms in equation (12). If the values of these terms can be separately determined from observational data, the relative importance of the physical processes can be ascertained.

Area and line integrals

Computations were made for an area based on the grid shown in Figure 1. Lines were drawn midway between rows and columns of grid points. Intersections of these lines formed 90 squares with a grid-point at the center of each square. Grid point values were assumed to be representative of the corresponding area increment, so that area integrals were approximated by summation over the grid, each value being weighted by the area involved.

The outer boundaries of the outermost squares form the perimeter of the modified area. The perimeter consists of 38 length increments. Under the assumption that a value assigned to the mid-point of a perimeter increment is representative of the entire increment, line integrals were approximated by summation over the perimeter, each value being weighted by the length involved.

Vertical integration

Vertical integration through the volume was approximated by the trapezoidal rule:

$$\int_{25\ mb}^{100mb} f(p)dp \doteq (25mb)\left[\frac{f(25) + f(50)}{2}\right] + (50mb)\left[\frac{f(50) + f(100)}{2}\right]$$

$$= (12.5mb)\,[f(25) + 3\,f(50) + 2\,f(100)] \qquad (14)$$

Input data

Details of the method of analysis and computational procedures to obtain the values of geopotential height Z, temperature T, the geostrophic wind components u and v, and of vertical motion ω at the 100-mb, 50-mb, and 25-mb levels have already been discussed in detail (Craig, Lateef, and Mitchem, 1961a, 1961b; Craig and Lateef, 1961, 1962). Only a brief summary of the procedures will, therefore, be given here.

The 100-mb maps were analyzed by conventional, subjective methods, including reference to off-time and off-level data whenever necessary and available. Careful attention was also paid to the geostrophic wind relationship. The heights of the 100-mb surface were considered to be boundary values which, along with the temperature distribution at higher levels determined the topography of higher-level pressure surfaces according to the hydrostatic relationship,

$$Z\,(x, y, p) = Z\,(x, y, p_0) + \frac{R}{g}\int_{p}^{p_0} T\,(x, y, p)\; d\,\ell n\; p$$

where Z is the height of a constant pressure surface in geopotential units and the other symbols have the usual meanings.

To determine the mean temperatures of the 100-mb to 50-mb and 50-mb to 25-mb layers, use was made of time-pressure cross sections prepared for all observing stations in the analysis area, about 130 in all.

The temperatures above 100 mb including those pertaining to the 50-mb and 25-mb surfaces were taken from the analyzed, smoothed cross sections and not directly from the published or original sources. The principal advantages to this were, firstly, any diurnal radiational errors were smoothed out and secondly, interpolation of missing data could be made with reasonable accuracy.

The base map used for all analyses was a polar stereographic projection with a scale of $1:2 \times 10^7$ at 60N. The values of height and temperature were read over the rectangular array of 132 points (Fig. 1) with a grid distance of 600 km at 60N and of 600 km $(1 + \sin \phi)/1.866$ at latitude ϕ.

All computations have been made for an x, y, p, t coordinate system, with the x-y plane tangent to the earth's surface at the location of the grid point for which the computation is made, and x and y positive in the directions indicated in Fig. 1. Directions x and y and geostrophic wind components u and v, therefore, point toward east and north only along the central column of grid points.

As with temperature, the errors in wind determination increase with height and are usually larger than in the troposphere, principally because the elevation angle of the sounding balloon is usually very small by the time the balloon reaches the tropopause level. In practice, considering the serious lack of data above 100 mb and the inaccuracies of the available measurements, it is assumed for most purposes that geostrophic equilibrium holds in the stratosphere. This assumption is reasonable in view of the scale of the systems involved. Muench (1958) has found the assumption to be entirely consistent with the available

data.

The computations of ω have been made from the adiabatic version of the first law of thermodynamics in the form,

$$\omega = \frac{\frac{\partial T}{\partial t} + u\frac{\partial T}{\partial x} + v\frac{\partial T}{\partial y}}{\varkappa\frac{T}{p} - \frac{\partial T}{\partial p}} \tag{15}$$

where $\varkappa$ is the ratio of the gas constant to the specific heat at constant pressure of dry air. The accuracy of computed vertical motions in the stratosphere, on the assumption of adiabatic temperature variations, has been discussed by Craig and Lateef (1962).

With the above approximations and with input data consisting of u, v, ω, Z, T for each grid point and of appropriate values for area and perimeter increments, it was possible to compute all the terms in equation (12) (except, of course, the dissipation term).

Finite difference approximations

The actual finite difference expressions used in the computations are as follows

$$\int_{p}^{p_0}\int_{A} k\, dA\, \frac{dp}{g} \doteq \frac{12.5\text{ mb}}{g}\left[\left(\sum_{i=1}^{90} k_i\Delta A_i\right)_{25\text{mb}} + 3\left(\sum_{i=1}^{90} k_i\Delta A_i\right)_{50\text{ mb}} + 2\left(\sum_{i=1}^{90} k_i\Delta A_i\right)_{100\text{ mb}}\right] \tag{16}$$

$$\frac{1}{g}\int_{p}^{p_0}\left(\oint_{L} k\, v_n\, dL\right)dp \doteq \frac{12.5\text{ mb}}{g}\left[\left(\sum_{j=1}^{38}\left(k\, v_n\right)_j \Delta L_j\right)_{25\text{ mb}} + 3\left(\sum_{j=1}^{38}\left(k\, v_n\right)_j \Delta L_j\right)_{50\text{ mb}} + 2\left(\sum_{j=1}^{38}\left(k\, v_n\right)_j \Delta L_j\right)_{100\text{ mb}}\right] \tag{17}$$

$$\frac{1}{g}\int_{p}^{p_0}\frac{\partial}{\partial p}\left(\int_A k\omega\, dA\right)dp \doteq \frac{1}{g}\left[\left(\sum_{i=1}^{90}(k\omega)_i\,\Delta A_i\right)_{100\text{ mb}} - \left(\sum_{i=1}^{90}(k\omega)_i\,\Delta A_i\right)_{25\text{ mb}}\right] \tag{18}$$

$$\frac{1}{g}\int_{p}^{p_0}\left(\oint_L \phi v_n\, dL\right)dp \doteq (12.5\text{ mb})\left[\left(\sum_{j=1}^{38}\left(Zv_n\right)_j\Delta L_j\right)_{25\text{ mb}} + 3\left(\sum_{j=1}^{38}\left(Zv_n\right)_j\Delta L_j\right)_{50\text{ mb}} + 2\left(\sum_{j=1}^{38}\left(Zv_n\right)_j\Delta L_j\right)_{100\text{ mb}}\right] \tag{19}$$

$$\frac{1}{g}\int_{p}^{p_0}\frac{\partial}{\partial p}\left(\int_A \phi\omega\, dA\right)dp \doteq \left[\left(\sum_{i=1}^{90}(Z\omega)_i\,\Delta A_i\right)_{100\text{ mb}} - \left(\sum_{i=1}^{90}(Z\omega)_i\,\Delta Ai\right)_{25\text{ mb}}\right] \tag{20}$$

$$\frac{R}{g}\int_{p}^{p_0}\left(\int_A \frac{\omega T}{p}\, dA\right)dp \doteq R\left(\frac{12.5\text{ mb}}{g}\right)\left[\frac{1}{25\text{ mb}}\left(\sum_{i=1}^{90}(\omega T)_i\,\Delta A_i\right)_{25\text{ mb}} + \frac{3}{50\text{ mb}}\left(\sum_{i=1}^{90}(\omega T)_i\,\Delta A_i\right)_{50\text{ mb}} + \frac{2}{100\text{ mb}}\left(\sum_{i=1}^{90}(\omega T)_i\,\Delta A_i\right)_{100\text{ mb}}\right] \tag{21}$$

In the above expressions, ΔL and ΔA refer to the perimeter and area increments respectively. v_n, the outward normal wind was evaluated as follows.

The average of the v components at grid points on the first row (Fig. 1) and corresponding points on the second row was taken as v_n through the northern boundary of the perimeter. A similar procedure was used for computing v_n through the southern boundary. In this case, however, the v components were used with change of sign to obtain the outward normal. Substitution of columns for rows and u's for v's,

yielded v_n at the eastern and western boundaries.

All computations were carried out on the IBM 709 computer at Florida State University.

Discussions concerning the specific results obtained in the evaluation of equations (16) to (21) for twice daily maps, at 0300 GCT and 1500 GCT for the period 0300 GCT of 17 January 1957 to 1500 GCT of 14 February 1957, are contained in Sections 6 to 11 of this report.

5. HEIGHT, TEMPERATURE AND VERTICAL MOTION PATTERNS

For the purpose of making the results of evaluation of the terms described in the previous section more understandable and as a guide to correlating variations in sign and magnitude of any of the terms with obvious changes in the synoptic pattern, a brief description of the warming will precede the presentation of the results. The evolution of the height, temperature and vertical motion fields during the course of the warming is described in this section.

Detailed presentation of the synoptic maps, spaced 48 hours apart, of height, temperature and vertical motion are contained in the published reports already referred to (Craig, Lateef and Mitchem, 1961a, 1961b; Craig and Lateef, 1961). Only a few of these maps are, therefore, shown in this report.

Figure 2 shows conditions on 17 January 1957, at the 100-mb, 50-mb and 25-mb surfaces before there was any obvious evidence of warming at any of these levels. A cold low existed at all levels, somewhere near the pole, skirted by a belt of strong westerlies. A trough extended southward from this low across the Hudson Bay and over the central United States at 100 mb and was displaced slightly to the east at the higher levels. The stratospheric warm belt was evident at 100 mb and 50 mb with relative temperature maxima at the trough. At 25 mb, the warm belt was not as evident as at the lower levels due to warmer temperatures in the tropical regions though the temperature field showed two weak maxima. At all levels, there was downward motion upstream from the trough and

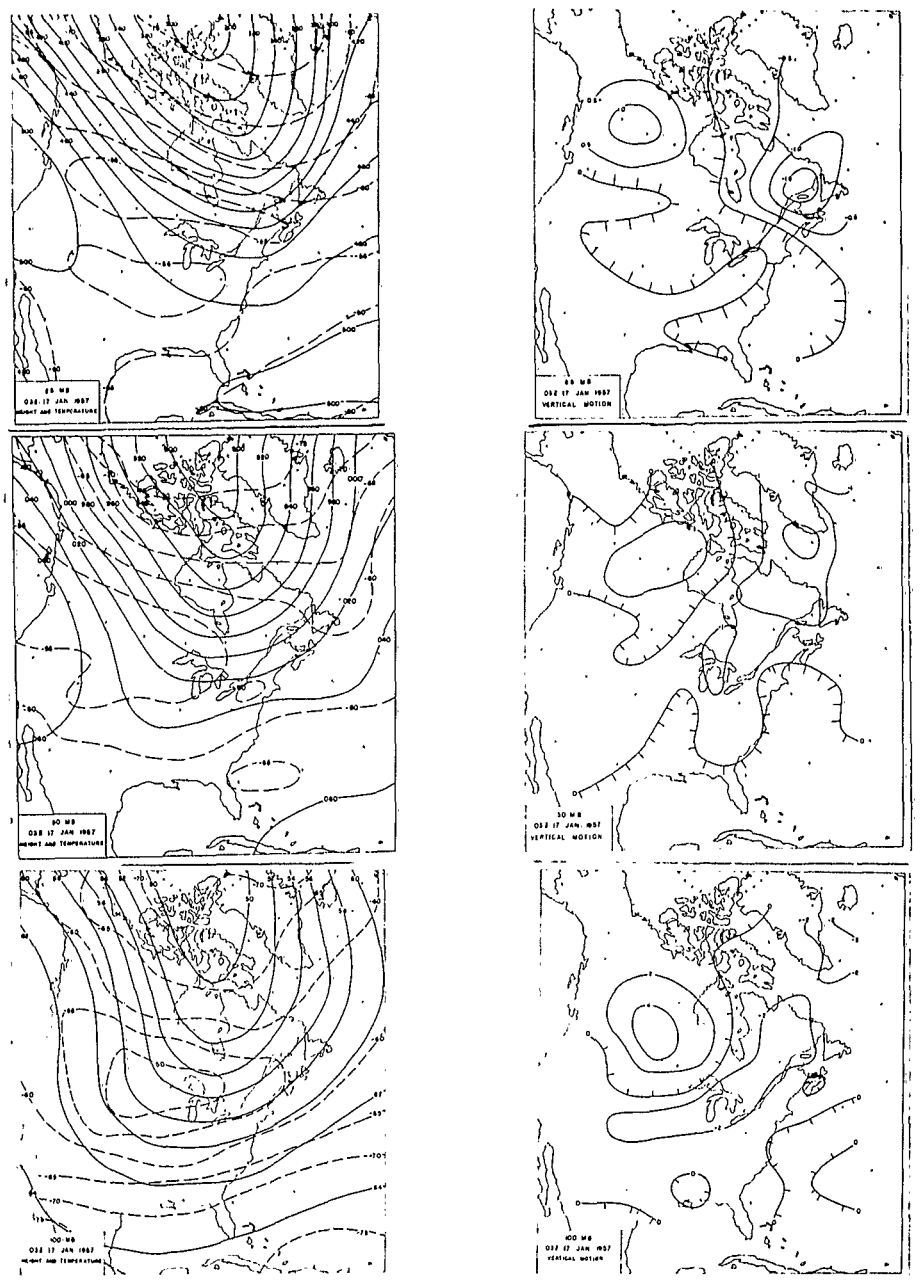

Fig. 2. Height, temperature and vertical motion patterns at 0300 GCT on 17 January, 1957. Contours are shown by solid lines and labeled in 100's of meters for 100 mb and in 10's of meters for 50 and 25 mb (with the initial digit omitted), isotherms by dashed lines and labeled in °C. Isopleths of ω are labeled in units of 10^{-1} dyne cm^{-2} sec^{-1}. Cross hatching on the zero isopleth of ω points toward downward motion.

upward motion downstream from the trough. Such a pattern of vertical motion is, of course, what one would expect if the trough is a region of relatively higher temperature and if the time rate of change of temperature is small compared to the advection term in the numerator of equation (15).

During the next few days the trough at 100 and 50 mb over the central United States, with its associated temperature maximum moved slowly eastward toward the North Atlantic. A new trough appeared at all levels, over the western United States by about 21 January. This trough remained almost stationary until about 2 February, when it began to retrogress northwestward. At 100 mb and 50 mb, this western trough was warm compared to downstream temperatures. In contrast, at 25 mb, temperatures increased in the direction of flow along this trough with no indication of a relative maximum at the trough axis.

The pattern of vertical motion at 100 mb and 50 mb during the period following 17 January and until about 2 February was characterized by two principal regions of ascent and descent in association with the two warm troughs. But the ω pattern at 25 mb underwent a radical change on and after 23 January in association with the formation and intensification of a warm center at this level. This warm center could be located off Nova Scotia on 25 January. Figure 3 shows conditions at all levels on this date and in particular the occurrence of downward motion at 25 mb over almost the entire analysis area. The large scale downward motion at 25 mb, initiated on 23 January persisted until near the end of the analysis period.

Changes in the contour height field at all levels and marked

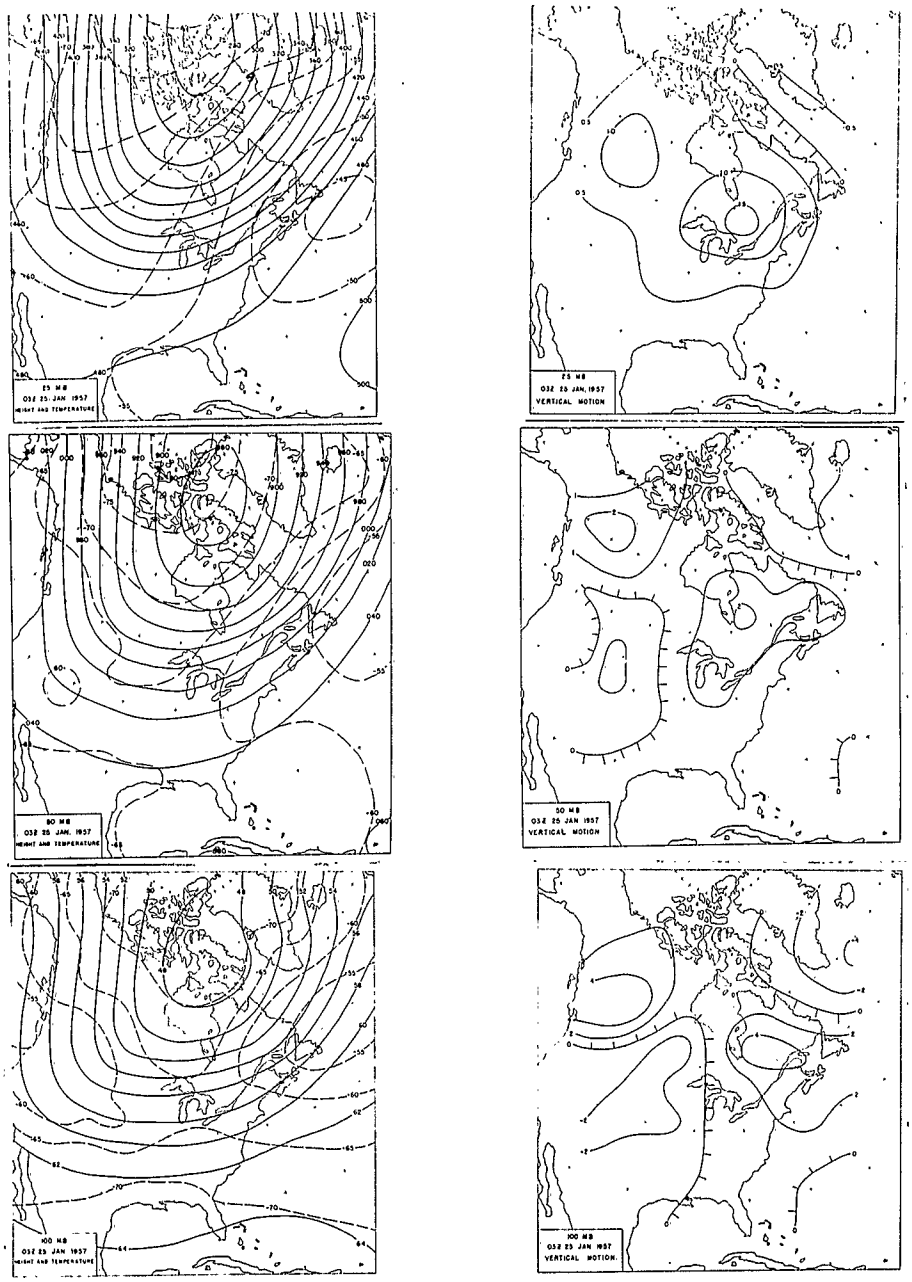

Fig. 3. Height, temperature and vertical motion patterns at 0300 GCT on 25 January, 1957. Contours are shown by solid lines and labeled in 100's of meters for 100 mb and in 10's of meters for 50 and 25 mb (with the initial digit omitted), isotherms by dashed lines and labeled in °C. Isopleths of ω are labeled in units of 10^{-1} dyne cm^{-2} sec^{-1}. Cross hatching on the zero isopleth of ω points toward downward motion.

developments in the temperature and vertical motion fields at 100 and 50 mb, began to take place after about 2 February. The cold polar vortex began to fill up and move westward giving rise to the establishment of east winds over the northern portions of the analysis area. The western United States trough slowly retrogressed northwestward and assumed cold characteristics at all three levels, with increasing temperatures both upstream and downstream.

The region of coldest temperature shifted from its previous location near the arctic low to the west or southwest of the low center. Pronounced warm centers could be located southeast of Greenland at 100 mb and south of Iceland at 50 mb, while an extension of the warming region towards the eastern United States was also evident. Figure 4 illustrates these changed conditions on 4 February. By this date, the 25-mb warm center which began its intensification on 23 January had reached its maximum with a central value of about -15C over southern Greenland. The 25-mb vertical motions had also reached their largest magnitudes. But radical changes had taken place in the ω fields at the lower levels. As seen in Fig. 4, the area covered by downward motion at these levels increased significantly and extended from the cold western trough to the warm eastern trough. This large scale motion persisted until near the end of the analysis period.

During the period 4 February to the end of the period, the low centered near Baffin Island continued to fill up rapidly and eventually showed up as a weak cyclonic circulation over the analysis area. The axis of the western United States trough which was retrogressing slowly, extended over Alaska towards the end of the period. The warm centers

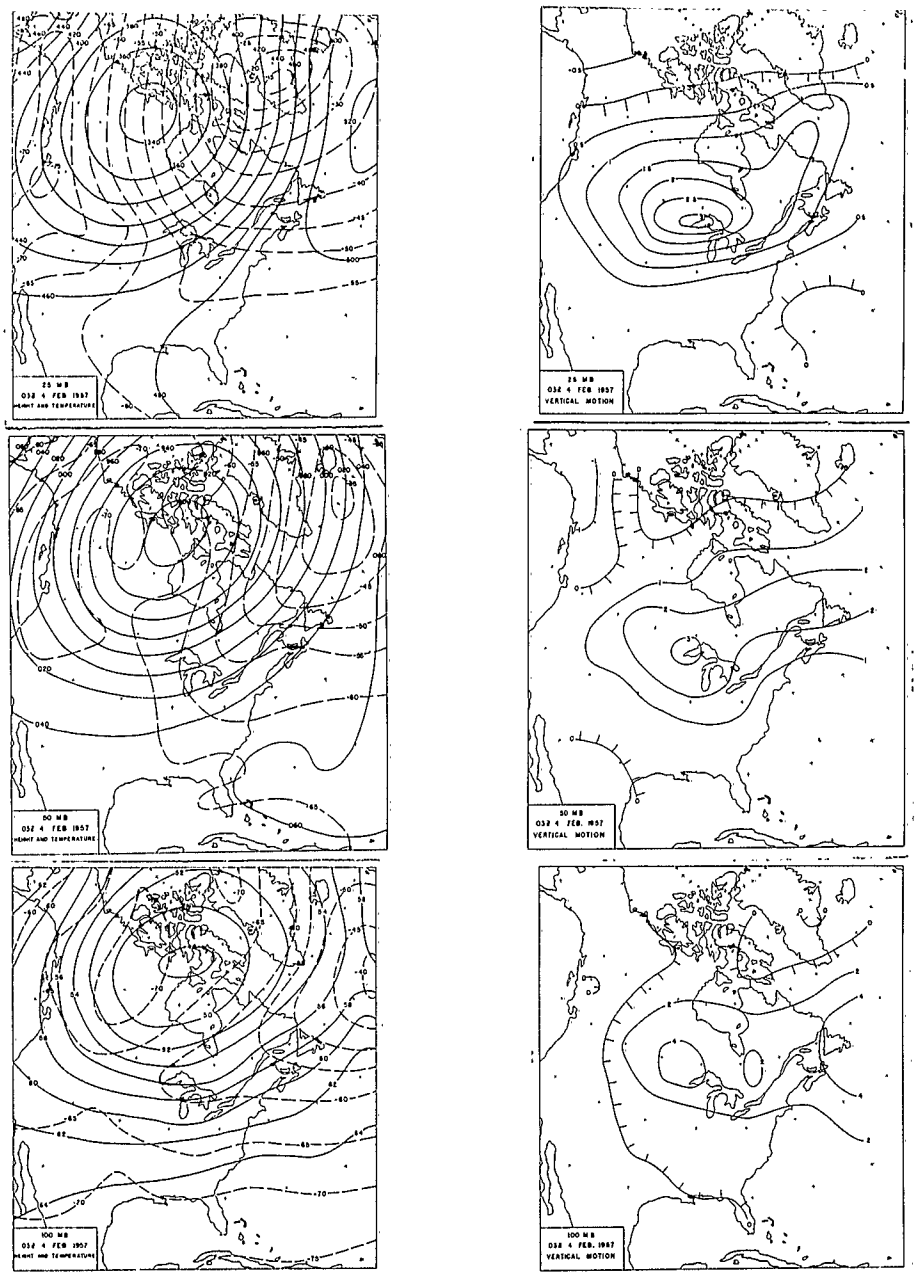

Fig. 4. Height, temperature and vertical motion patterns at 0300 GCT on 4 February, 1957. Contours are shown by solid lines and labeled in 100's of meters for 100 mb and in 10's of meters for 50 and 25 mb (with the initial digit omitted), isotherms by dashed lines and labeled in °C. Isopleths of ω are labeled in units of 10^{-1} dyne cm^{-2} sec^{-1}. Cross hatching on the zero isopleth of ω points toward downward motion.

at the lower levels also moved towards the northwest and later toward the west. By the end of the period (Fig. 5), the north south temperature gradient at all levels was completely reversed from that prevailing in mid-January. The vertical motion pattern at all levels was marked by two regions of ascent and descent, generally over the western and eastern halves of the continent, a reversal of the pattern on 17 January.

The significance of the changes in the vertical motion patterns that occurred at 25 mb by about 25 January and at the lower levels after about 2 February, has been discussed by Craig and Lateef (1962). They have pointed out that the important difference between vertical motions prior to and after about 23 January at 25 mb and before and after 2 February at the lower levels lay in the scale of downward motion at these levels, rather than in any large changes in their magnitude. The preponderance of such motion at 25 mb on 25 January (Fig. 3) and its occurrence at 100 and 50 mb on 4 February (Fig. 4) illustrate the large scale of downward motion during the stratospheric warming.

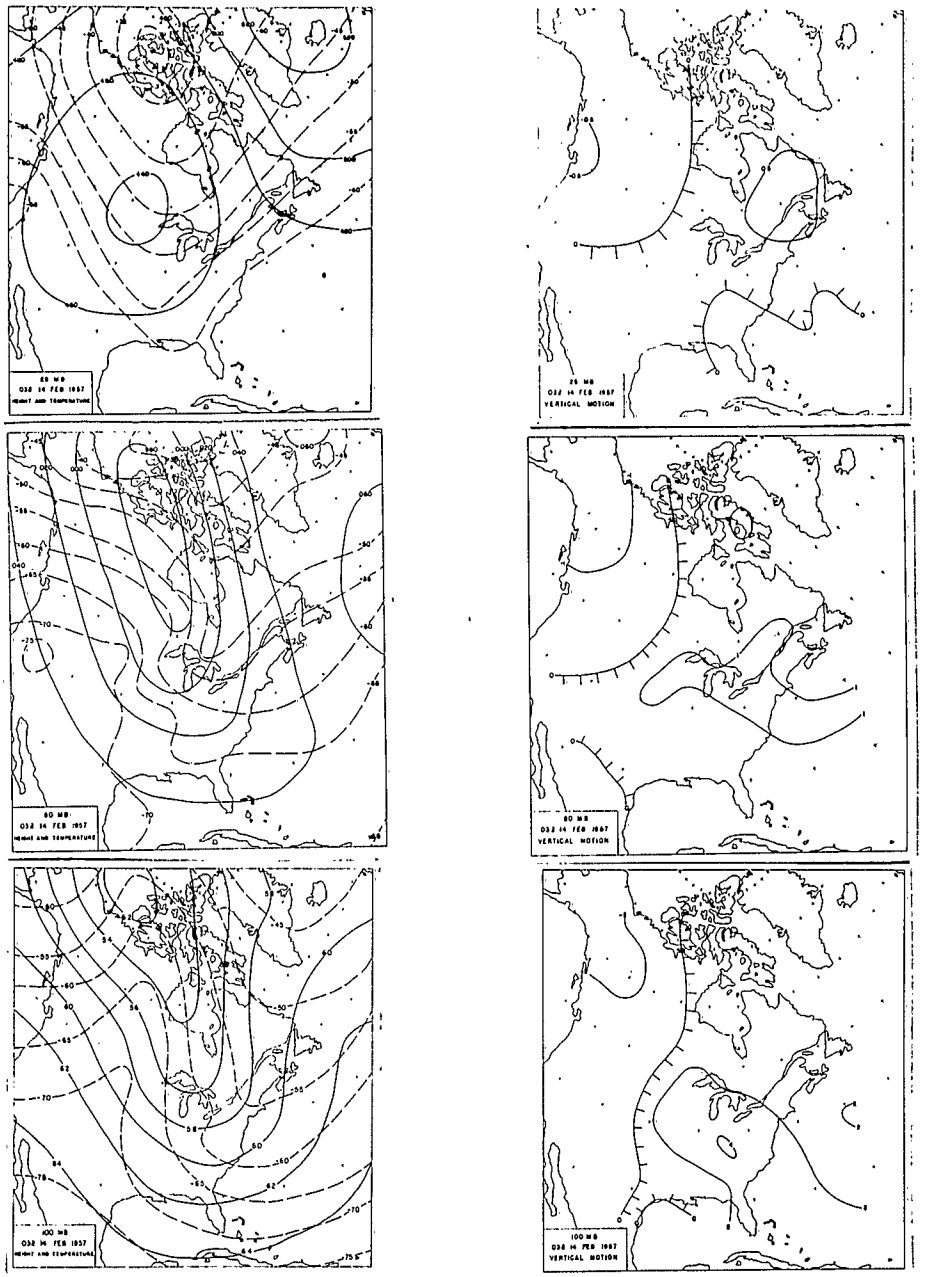

Fig. 5. Height, temperature and vertical motion patterns at 0300 GCT on 14 February, 1957. Contours are shown by solid lines and labeled in 100's of meters for 100 mb and in 10's of meters for 50 and 25 mb (with the initial digit omitted), isotherms by dashed lines and labeled in °C. Isopleths of ω are labeled in units of 10^{-1} dyne cm^{-2} sec^{-1}. Cross hatching on the zero isopleth of ω points toward downward motion.

6. VARIATION OF KINETIC ENERGY IN THE VOLUME

It is, first of all, of interest to consider how the kinetic energy actually varied during the period. The volume integral of kinetic energy denoted by K on the left side of equation (12) was evaluated twice daily for the entire volume as well as for the 100-50 mb and 50-25 mb layers. Figure 6 shows the variation of K with time during the period while Figures 7 and 8 show the variation of kinetic energy within the layers.

The values of K have been somewhat smoothed by the application of an elementary binomial smoothing function with weights 1/4, 1/2, 1/4. This type of smoothing eliminates fluctuations in the values due to any diurnal variations and random errors. Following a technique used by Shuman (1957) it can be shown that the amplitudes of any variations of wave components with periods much longer than 24 hours are not seriously affected by this smoothing process. A smoothed element $\overline{K}$ defined as above, is denoted by

$$\overline{K} = \frac{1}{4} K_{t-12\ hr} + \frac{1}{2} K_t + \frac{1}{4} K_{t+12\ hr} \qquad (22)$$

With such a definition, σ, the factor by which the amplitudes of the smoothed values of each wave component are reduced is given by

$$\sigma = \frac{1 + \cos \mu h}{2} \qquad (23)$$

where μ is the wave number and h is the length of the finite difference

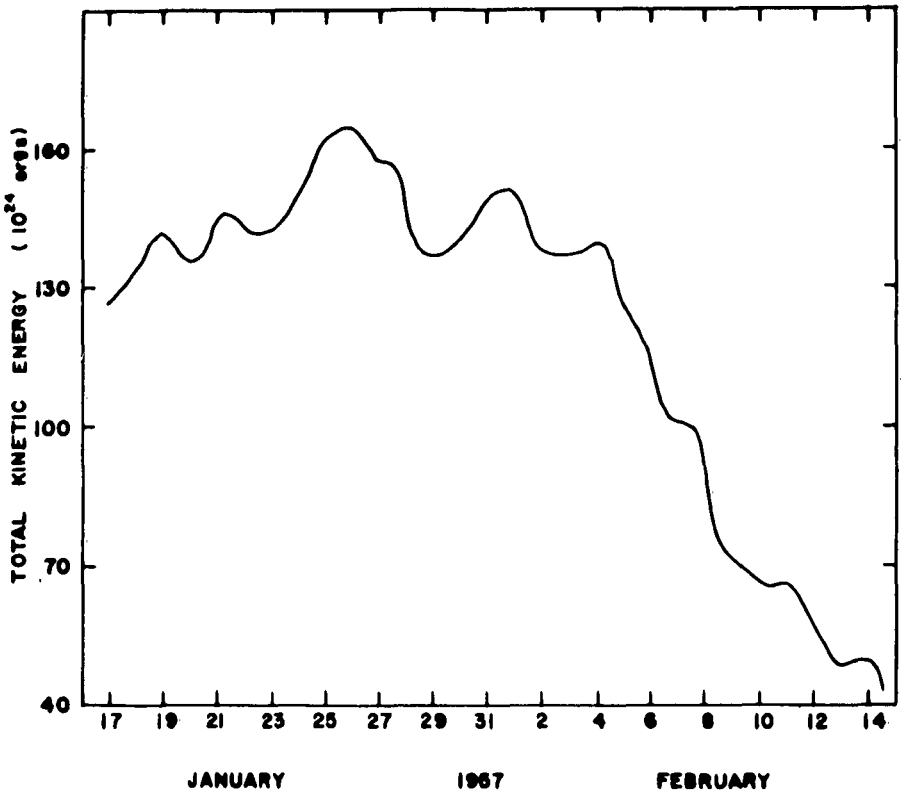

Fig. 6. Variation with time of the total kinetic energy in the volume, bounded by the perimeter of the grid and the 100-mb and 25-mb pressure surfaces.

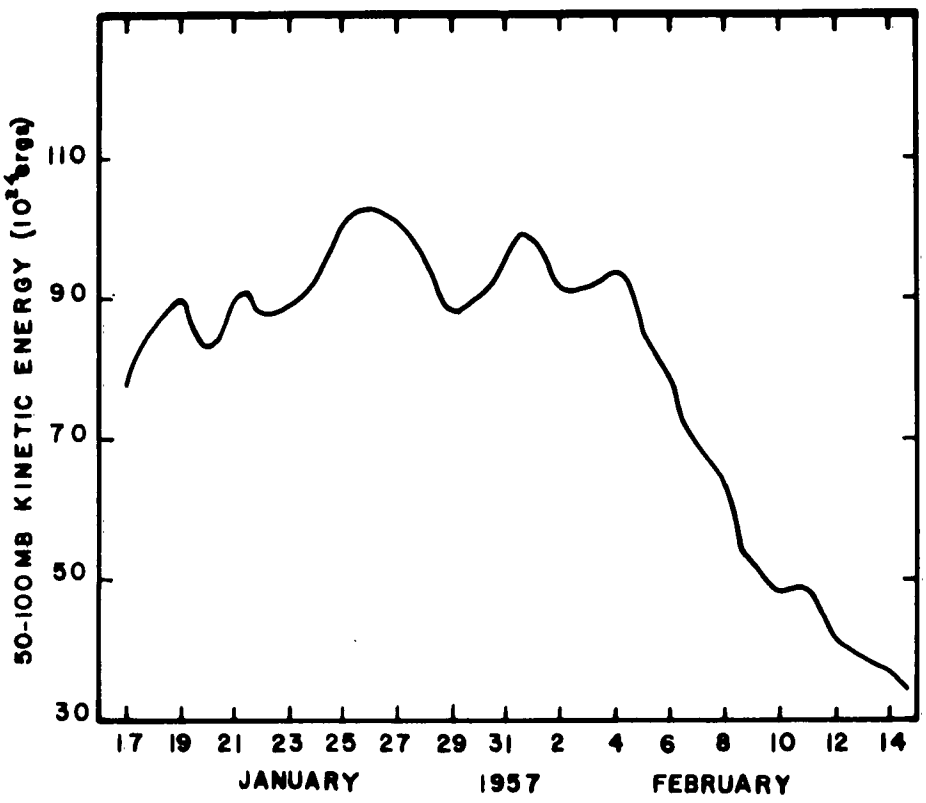

Fig. 7. Variation with time of the kinetic energy in the layer, bounded by the perimeter of the grid and the 100-mb and 50-mb pressure surfaces.

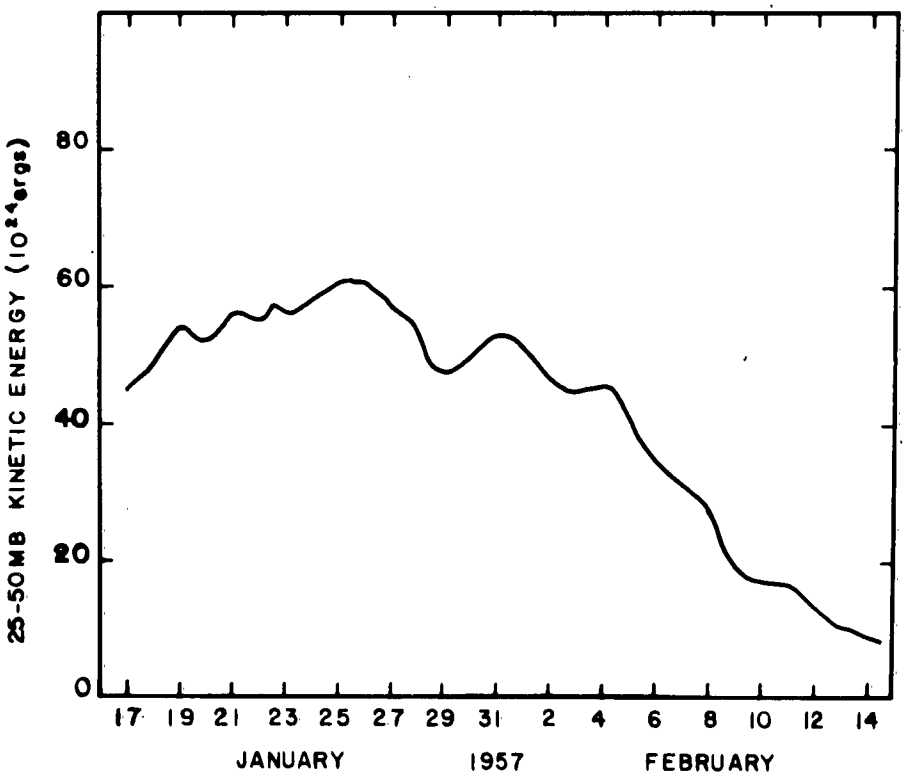

Fig. 8. Variation with time of the kinetic energy in the layer, bounded by the perimeter of the grid and the 50-mb and 25-mb pressure surfaces.

increment in K. In our case h = 12 hours, since the values of K are given 12 hours apart. According to equation (23), components of wavelength 10 h, that is, variations in K due to fluctuations with periods of 5 days, would be reduced only by 10 per cent.

The time variations in kinetic energy exhibited in Figs. 6, 7 and 8 are almost identical in nature. Increases and decreases in kinetic energy both for the volume and for the two layers treated separately, occurred simultaneously. These figures suggest four time periods into which the data might be subdivided for further study.

(a) From 17 January to about 25 January, K showed a gradual increase, with shorter period fluctuations superimposed. This was the period during which a trough over the central United States moved eastwards to the North Atlantic while a new trough appeared over the southwestern United States. The warming at 25 mb had just begun towards the end of this period but there was no evidence of warming at the lower levels.

(b) From 26 January to about 3 February, K showed a general decrease. This was the period when the warming was apparent at 25 mb, but not yet throughout the entire volume. The cyclonic center over Baffin Island was slowly filling up at all the three levels.

(c) From 4 February to about 8 February, K decreased very rapidly. This was the period when rapid temperature increases were taking place at 50 mb and 100 mb. The warm center at 25 mb maintained its intensity until 6 February but later started to weaken. The cold cyclonic vortex which remained nearly vertical until 3 February, began a definite westward movement during this period.

(d) From 9 February to the end of the period, K continued to decrease, but less rapidly. This was the period when the rapid temperature changes had already occurred and the north south temperature gradient at all levels was reversed from that prevailing in mid-January. The polar vortex with its belt of westerlies was replaced by a weak cyclonic circulation over the United States with easterlies over the polar regions.

The values of K for the volume are given in Table 1. From these values, the magnitudes of $\partial K/\partial t$ computed for the 4 periods mentioned above, are given in Table 2.

Table 1. Kinetic energy of the volume, in units of 10^{24} ergs.

Date	Time (GCT)	K
17 January	0300	127
	1500	130
18	0300	133
	1500	140
19	0300	144
	1500	139
20	0300	135
	1500	137
21	0300	145
	1500	147
22	0300	143
	1500	142
23	0300	143
	1500	145
24	0300	149
	1500	157
25	0300	163
	1500	164
26	0300	164
	1500	162
27	0300	157
	1500	156

Table 1. Continued

Date	Time (GCT)	K
28 January	0300	149
	1500	138
29	0300	136
	1500	139
30	0300	140
	1500	144
31	0300	150
	1500	152
1 February	0300	151
	1500	143
2	0300	138
	1500	137
3	0300	137
	1500	137
4	0300	140
	1500	136
5	0300	126
	1500	120
6	0300	115
	1500	104
7	0300	100
	1500	100
8	0300	91
	1500	77
9	0300	71
	1500	69
10	0300	67
	1500	66
11	0300	66
	1500	65
12	0300	57
	1500	52
13	0300	49
	1500	50
14	0300	51
	1500	44

Table 2. Average values of $\partial K/\partial t$, in units of 10^{24} ergs per hour.

Period	$\partial K/\partial t$
17 January to 25 January	0.23
25 January to 4 February	-0.09
4 February to 9 February	-0.57
9 February to 14 February	-0.19

A comparison of these rates of change in kinetic energy with estimates made by Wolfe (1960) shows that these values are comparable to those on a hemispheric scale. Wolfe estimated $\partial K/\partial t$ at 50 mb to be about -3.2 ergs cm^{-2} mb^{-1} sec^{-1} for the period 25 January to 9 February 1957 over a large portion of the Northern Hemisphere. The corresponding rate of change of kinetic energy in the 100-50 mb layer for the limited volume in the present study is -2.8 ergs cm^{-2} mb^{-1} sec^{-1}.

No attempt has been made in the present study to subdivide the kinetic energy of the volume into zonal and eddy components. With the limited longitudinal extent of the volume, such an attempt is considered neither useful nor meaningful. It is interesting to note, however, that Wolfe's computations showed that $\partial K/\partial t$ was actually positive in latitudes north of 65N. The areas dominated by the negative rate of change of kinetic energy south of 65N were much larger than those under the influence of the positive rate of change, with the result that $\partial K/\partial t$ assumed an overall negative value.

7. HORIZONTAL AND VERTICAL ADVECTION OF KINETIC ENERGY

The horizontal advection of existing kinetic energy across the vertical boundaries of the volume is represented by the (kv_n) term of Section 2. Change in kinetic energy within the volume due to vertical transport of existing kinetic energy through the constant pressure surfaces, is given by the $(k\omega)$ term.

Horizontal advection of kinetic energy

Parcels of air possessing kinetic energy are displaced horizontally into or out of the volume by the wind components normal to the perimeter. This leads to changes in the kinetic energy of the volume. Computations of such changes, brought about by horizontal advection of existing kinetic energy, were made according to the finite difference approximation procedure shown in equation (17). The method of estimation of the values for v_n over each perimeter increment has already been described in Section 4. Values of k on the perimeter could not, however, be computed because the geostrophic wind relationship gave only the u components along the first and twelfth rows of the original grid of 132 points (Fig. 1) and only the v components along the first and eleventh columns. In place of the values of k on the perimeter, the kinetic energies already computed over the area increments for use in equation (16) were assigned to the corresponding perimeter increments in equation (17). Such a procedure is satisfactory enough. On the assumption of a 10 per cent error in u and v and a corresponding error in k due to this

procedure, it can be shown that, in the extreme case of v_n being of the same sign all along the perimeter, the error introduced in the evaluation of $\Sigma (kv_n)_j \Delta L_j$ is less than 1 per cent.

The rates of change of kinetic energy in the volume due to horizontal flux of kinetic energy across the vertical boundaries, are listed in Table 3. Except in the beginning of the period, the horizontal flux consistently acted to decrease the kinetic energy of the volume until about 3 February. After this date and until the end of the analysis period, this process acted to increase K. The rates of decrease in K were generally higher than the rates of increase.

Values of the horizontal advection term for the 100-50 mb layer and 50-25 mb layer at each map time also indicated that this term was negative, that is, acted to decrease kinetic energy, in both the layers up to 3 February and was positive thereafter. These values are not included in this report.

Table 3. Rate of change of kinetic energy of the volume due to advection of kinetic energy, in units of 10^{21} ergs per second.

Date	Time (GCT)	(kv_n)	$(k\omega)$
17 January	0300	0.24	0.02
	1500	0.19	0.03
18	0300	0.04	0.03
	1500	-0.16	0.02
19	0300	-0.20	0.01
	1500	-0.13	0.01
20	0300	-0.16	0.02
	1500	-0.24	-0.01
21	0300	-0.28	-0.02
	1500	-0.28	-0.01
22	0300	-0.25	0.03
	1500	-0.23	0.07

Table 3. Continued

Date	Time (GCT)	(kv_n)	($k\omega$)
23 January	0300	-0.19	0.10
	1500	-0.15	0.10
24	0300	-0.21	0.07
	1500	-0.27	0.02
25	0300	-0.26	0.00
	1500	-0.25	0.03
26	0300	-0.26	0.05
	1500	-0.31	0.03
27	0300	-0.35	0.00
	1500	-0.39	0.00
28	0300	-0.46	0.02
	1500	-0.54	0.02
29	0300	-0.51	0.02
	1500	-0.41	0.02
30	0300	-0.34	0.01
	1500	-0.29	0.03
31	0300	-0.26	0.09
	1500	-0.32	0.10
1 February	0300	-0.39	0.07
	1500	-0.35	0.05
2	0300	-0.28	0.01
	1500	-0.21	-0.01
3	0300	-0.10	-0.01
	1500	0.02	-0.03
4	0300	0.17	-0.01
	1500	0.26	-0.15
5	0300	0.22	-0.15
	1500	0.19	-0.17
6	0300	0.20	-0.19
	1500	0.17	-0.19
7	0300	0.15	-0.20
	1500	0.17	-0.23
8	0300	0.16	-0.20
	1500	0.10	-0.16
9	0300	0.06	-0.14
	1500	0.06	-0.11
10	0300	0.07	-0.11
	1500	0.13	-0.13
11	0300	0.16	-0.14
	1500	0.16	-0.12
12	0300	0.15	-0.10
	1500	0.10	-0.08
13	0300	0.05	-0.08
	1500	0.04	-0.09
14	0300	0.04	-0.09
	1500	0.03	-0.08

Since the u and v components were computed geostrophically, the values obtained for the horizontal flux actually represent only the flux of geostrophic kinetic energy owing to the geostrophic wind components. The actual kinetic energy may be considered very nearly equal to that computed with geostrophic winds. But the real flux may be different, as there would be departures from the actual wind both in magnitude and direction. Unfortunately, in the absence of extensive wind observations, it is impossible to know these departures. Estimates of the magnitudes of the errors introduced in the computation of the advection term, using geostrophic v_n can however, be made with sufficient confidence. Such estimates were not made because this term turned out to be relatively unimportant in the kinetic energy budget of the volume. A comparison of the magnitudes of the advection term with those of the generation terms is shown in Section 11. The extra effort in re-evaluating the advection term was, therefore, considered unnecessary.

The values of the rate of change of kinetic energy in the volume due to horizontal advection, for the four time periods mentioned in Section 7, are contained in Table 4.

Table 4. Average values of (kv_n) and $(k\omega)$, in units of 10^{24} ergs per hour.

Period	(kv_n)	$(k\omega)$
17 January to 25 January	-0.57	0.12
25 January to 4 February	-1.08	0.08
4 February to 9 February	0.63	-0.64
9 February to 14 February	0.33	-0.38

Vertical advection of kinetic energy

The rates of change of kinetic energy in the volume due to a net flux of kinetic energy from the adjacent layers above and below the boundary pressure surfaces, were computed according to equation (18). Results of the computations are included in Table 3.

The most obvious feature of these results is the occurrence of consistently negative values after 2 February until the end of the period. During approximately the same period, the (kv_n) values were consistently positive and of comparable magnitude.

The values of the vertical advection term were predominantly positive from 17 January to 2 February. The group of small negative values around 20 January could, perhaps, be attributed to errors in data particularly at the boundaries of the analysis area.

The values for the rate of change of kinetic enegy in the 100-50 mb and 50-25 mb layers owing to vertical advection of existing kinetic energy above and below these layers (not included in this report) were also computed using equation (18) with the appropriate pressure boundary values. Until about 31 January, the values for the two layers treated separately, did not show any consistent pattern as regards their individual contributions to the rate of change of kinetic energy in the volume. Between 31 January and 2 February, the downward transport of kinetic energy through the 25-mb pressure surface exceeded the amount through the 50-mb surface while the downward transport through 100 mb was less than at 50 mb (Fig. 9). Thus, there was a positive contribution to the rate of change of kinetic energy in both the layers, amounting to a substantial positive rate for the volume. The combined

contribution from the vertical advection process through both the layers resulted in the group of relatively high positive values in Table 3 for this period.

After about 2 February and until the end of the period, the magnitudes of the downward transport of kinetic energy through the three pressure surfaces increased with depth (Fig. 9). The result was a negative contribution to the rate of change of kinetic energy in both the 100-50 mb and 50-25 mb layers. For the volume, the downward transport through 100 mb exceeded the downward transport through 25 mb, so that the vertical advection process consistently acted to decrease the volume kinetic energy. The vertical motion patterns at the three pressure levels, after 2 February, show that these negative values could be largely attributed to the radical changes that took place in the ω field at the 50 and 100-mb levels. As illustrated in Fig. 4, the area of downward motion at these levels began to increase significantly, about this time. The establishment of a larger scale of downward motion at these levels, rather than any substantial changes in the magnitudes of ω, was apparently responsible for the observed negative contribution to $\partial K/\partial t$, due to net vertical transport of energy through the volume.

The values of the rate of change of volume kinetic energy due to vertical advection, for the four chosen time periods, are listed in Table 4.

A comparison of the values of (kv_n) and $(k\omega)$ in Tables 3 and 4 indicates an apparent tendency for these two terms to compensate each other. In the presence of processes generating and dissipating kinetic energy in the volume, there is no obvious reason to consider kinetic

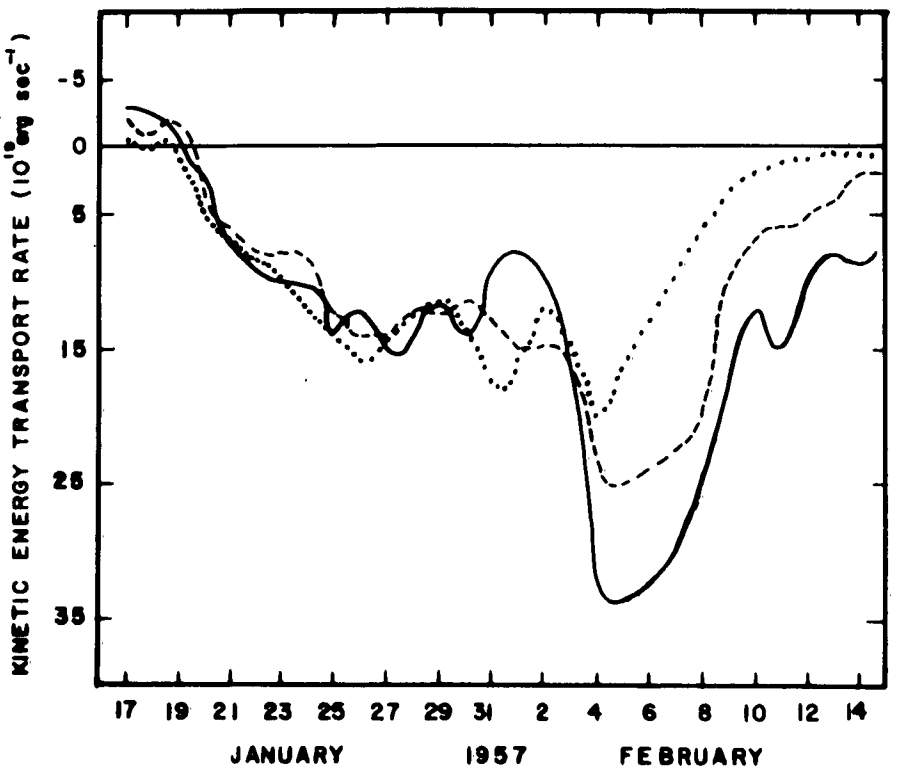

Fig. 9. Vertical transport rate of kinetic energy through the 100-mb (solid line), 50-mb (dashed line) and 25-mb (dotted line) levels. Positive values signify downward transport of kinetic energy.

energy to be locally conserved. Any net horizontal advection of kinetic energy into or out of the volume through the vertical boundaries, need not, per se, bring about a compensating vertical flux of existing kinetic energy through the horizontal boundaries. It is interesting to note, however, that Jensen (1960) has also indicated the same compensating tendencies between horizontal convergence and vertical transport of kinetic energy in the lower troposphere over the Northern Hemisphere. It would appear therefore, that the apparent compensation among the transport processes alone, could be a general characteristic of the atmosphere and not a consequence of the conditions in the limited volume under study.

8. GENERATION OF KINETIC ENERGY AT THE BOUNDARIES

The contributions to the rate of change of kinetic energy in the volume due to generating processes acting on the boundaries are represented by the terms (c) and (d) specified in Section 2. Term (c), namely, $-\frac{1}{g}\int_{p}^{p_0}(\phi_L\, \phi v_n\, dL)\, dp$, gives the rate of generation of kinetic energy through horizontal motions across the vertical boundaries of the volume. Term (d), namely, $\frac{1}{g}\left[\left(\int_A (\phi\omega)\, dA\right)_p - \left(\int_A (\phi\omega)\, dA\right)_{p_0}\right]$ gives the rate of generation of kinetic energy through vertical motions at the boundary pressure surfaces.

Generation of kinetic energy at the vertical boundaries

The rate of change of kinetic energy in the volume due to the (ϕv_n) process was computed according to the finite difference summation procedure shown in equation (19). The values of the geopotential heights at the grid points just inside the analysis area (Fig. 1) were assigned to the perimeter increments. The error in the evaluation of the term $\Sigma\,(Zv_n)_j\,\Delta L_j$, in equation (19), at any pressure level, by not using Z's along the perimeter itself, amounted to less than 1 per cent, even under assumption of extreme situations.

Initially, the geostrophic v_n's already computed as described in Section 4, were used for the evaluation of the (ϕv_n) term for the volume, for each map time. This computation gave the contribution to the (ϕv_n) process from the displacements of ϕ at the boundary due to the geostrophic wind components. Since the generation process is mathematically

equivalent to a flux or transfer rate of potential energy, the above computation gave only the geostrophic flux of potential energy. The real flux might be different, to the extent the actual wind departed from the geostrophic value. In the absence of actual observed winds at a sufficiently large number of stations along the perimeter, only a reasonably close estimate could be made of the true flux. The method of estimating the flux due to the ageostrophic component was as described below.

The ageostrophic flux of potential energy

Since v_n can be represented as $v_n = v_{ng} + v_{na}$, where v_{ng} and v_{na} are the geostrophic and ageostrophic normal wind components, we may write

$$\left(\phi v_n\right) = \left(\phi v_{ng}\right) + \left(\phi v_{na}\right) \tag{24}$$

The ageostrophic flux of potential energy is represented by the term

$$\left(\phi v_{na}\right) = -\frac{1}{g}\int_{p}^{p_0}\left(\oint_L \phi v_{na}\, dL\right) dp = -\int_{p}^{p_0}\left(\oint_L Z v_{na}\, dL\right) dp \tag{25}$$

Let $\overline{\ }$ denote mean over L, so that

$$\overline{(\ )} = \frac{1}{L}\oint_L (\ )\, dL \doteq \frac{1}{L}\left[\sum_{j=1}^{38} (\ )_j\, \Delta L_j\right] \tag{26}$$

and

$$\left(\phi v_{na}\right) = -L\int_{p}^{p_0} \overline{Z v_{na}}\, dp \tag{27}$$

The evaluation of $\overline{Z v_{na}}$ required knowledge of v_{na} over each perimeter increment. This was not available in the absence of actual wind

observations along the perimeter. The following procedure was therefore adopted to obtain a close estimate of (ϕv_{na}) for the volume.

The averaging of the values of the product of Z and v_{na} along the perimeter can also be expressed as

$$\overbrace{Zv_{na}} = \tilde{Z}\,\tilde{v}_{na} + \overbrace{Z'v'_{na}} \tag{28}$$

where the primed quantities denote departures of Z and v_{na} over each perimeter increment, from their peripheral mean values.

In what follows, the method of obtaining the mean term $\tilde{Z}\,\tilde{v}_{na}$ is described. It will be shown that the term $\overbrace{Z'v'_{na}}$ could be neglected as being at least an order of magnitude smaller than the mean term.

The computation of $\tilde{v}_{na}$ and $\tilde{Z}$

From the relations

$$L\,\tilde{v}_n = L\,\tilde{v}_{ng} + L\,\tilde{v}_{na} \tag{29}$$

$$\int_p^{p_0}\left(\int_A \nabla \cdot \underline{V}\, dA\right) dp = -\int_p^{p_0} \frac{\partial}{\partial p}\left(\int_A \omega\, dA\right) dp \tag{30}$$

and

$$\int_A \nabla \cdot \underline{V}\, dA = \oint_L v_n\, dL = L\,\tilde{v}_n \tag{31}$$

it follows that $\tilde{v}_{na}$ can be computed from $\tilde{v}_n$ given by equations (30) and (31) and from $\tilde{v}_{ng}$ obtained through the geostrophic u and v components across the perimeter increments.

However, equation (30) implies that the values of $\tilde{v}_n$ would essentially apply to the mean pressure height of the layer through which the

integration is carried out. Hence $\overline{v_n}$ for the 100-50 mb layer and $\overline{v_n}$ for the 50-25 mb layer were computed separately and these values of $\overline{v_n}$ were considered to apply at 75-mb and 37.5-mb levels respectively. $\overline{v_{ng}}$ at 75 mb was taken to be the mean of $\overline{v_{ng}}$ at 100 mb and 50 mb and $\overline{v_{ng}}$ at 37.5 mb to be the mean of values at 50 and 25 mb. Using the values of $\overline{v_n}$ and $\overline{v_{ng}}$ at 75 and 37.5 mb, $(\overline{v_{na}})_{75mb}$ and $(\overline{v_{na}})_{37.5mb}$ were computed for each map time.

The next step was to obtain the geopotential height Z at 75 mb and 37.5 mb. On the assumption of a logarithmic relationship between height and pressure, the following approximations were used to get Z_{75mb} and $Z_{37.5mb}$.

$$\overline{Z_{75mb}} = \overline{Z_{100mb}} + \frac{\ell n\ 10 - \ell n\ 7.5}{\ell n\ 10 - \ell n\ 5}\left[\overline{Z_{50mb}} - \overline{Z_{100mb}}\right]$$

$$= 0.585\ \overline{Z_{100mb}} + 0.415\ \overline{Z_{50mb}} \qquad (32)$$

Similarly,

$$\overline{Z_{37.5mb}} = 0.585\ \overline{Z_{50mb}} + 0.415\ \overline{Z_{25mb}} \qquad (33)$$

Having obtained $\overline{Z}$ and $\overline{v_{na}}$ at 75 mb and 37.5 mb, the contribution to the (ϕv_n) process of the term $L\ \overline{Z}\ \overline{v_{na}}$ could be computed.

For the 100-50 mb layer, this term amounted to 50 mb $L\left(\overline{Z}\ \overline{v_{na}}\right)_{75mb}$ and for the 50-25 mb layer, it amounted to 25 mb $L\left(\overline{Z}\ \overline{v_{na}}\right)_{37.5mb}$. The sum of these two terms gave an estimate of the contribution to the (ϕv_n) process due to the ageostrophic wind components.

Though the term $\overline{Z'v'_{na}}$ of (28) could not be evaluated in the absence of actual wind observations, it is possible to estimate the

relative order of magnitude of this term as compared to $\overline{Zv_{ng}}$.

As part of the computations of $\overline{Z}$, the values of Z' over each perimeter increment were also obtained. These values indicated that the maximum value of Z' at any level did not exceed 500 meters, during the period. Reference to the order of magnitude of the values of $L\ \overline{Zv_{ng}}$ term at any level, showed that these values were of the order of 10^{18} cm^3 sec^{-1}. Hence, in order that $\overline{Z'v'_{na}}$ should make a sizeable contribution to the (ϕv_n) process, the integrated value, $L\ \overline{Z'v'_{na}}$, should be of the same order of magnitude. Knowing the maximum value of Z', the magnitude of v'_{na} corresponding to a value for $L\ \overline{Z'v'_{na}}$ of say, 10^{17} cm^3 sec^{-1}, can be ascertained.

Let ΔL = 540 km, an average value. Then $L\ \overline{Z'v'_{na}} \doteq \sum_{j=1}^{38} \left(Z'v'_{na}\right)_j \Delta L_j = 10^{17}$ cm^3 sec^{-1}, or

$$38\ (5 \times 10^4\ cm)\ (v'_{na})\ (5.4 \times 10^7\ cm) = 10^{17}\ cm^3\ sec^{-1}.$$

Thus v'_{na} should be at least 10 meters per second, over every perimeter increment, each one of them having Z' = 500 meters. It is difficult to visualize a departure of v'_{na} of this magnitude acting in the same direction all around the perimeter at all levels, together with the unrealistic extreme departure Z' of 500 meters over every perimeter increment. The contribution of $\overline{Z'v'_{na}}$ to the (ϕv_n) process may, therefore, be neglected.

Table 5 gives the values of the (ϕv_{ng}) term, the (ϕv_{na}) term and the sum of these two terms representing the rate of change of kinetic energy in the volume due to the (ϕv_n) process.

Table 5. Rate of change of kinetic energy of the volume due to the (ϕv_n) process, in units of 10^{21} ergs per second.

Date	Time (GCT)	(ϕv_{ng})	(ϕv_{na})	(ϕv_n)
17 January	0300	-16.85	7.96	-8.89
	1500	-10.53	3.98	-6.55
18	0300	-5.69	0.1	-5.59
	1500	-1.45	-1.71	-3.16
19	0300	3.51	-3.63	-0.12
	1500	7.61	-7.03	0.58
20	0300	9.57	-8.35	1.22
	1500	11.91	-8.25	3.66
21	0300	14.54	-11.15	3.39
	1500	16.57	-16.20	0.37
22	0300	16.91	-18.48	-1.57
	1500	13.36	-16.43	-3.07
23	0300	8.45	-13.29	-4.84
	1500	6.69	-11.87	-5.18
24	0300	8.45	-11.06	-2.61
	1500	9.94	-8.26	1.68
25	0300	7.69	-4.71	2.98
	1500	4.47	-4.20	0.27
26	0300	3.77	-6.53	-2.76
	1500	2.62	-6.90	-4.28
27	0300	-3.09	-2.22	-5.31
	1500	-9.96	2.31	-7.65
28	0300	-10.15	0.51	-9.64
	1500	-6.24	-5.53	-11.77
29	0300	-3.34	-4.85	-8.19
	1500	-1.94	-1.96	-3.90
30	0300	-0.99	-3.72	-4.71
	1500	-1.89	-5.42	-7.31
31	0300	-6.26	-2.74	-9.00
	1500	-6.56	-2.57	-9.13
1 February	0300	-2.58	-5.77	-8.35
	1500	-0.31	-6.90	-7.21
2	0300	2.44	-5.23	-2.79
	1500	8.37	-5.75	2.62
3	0300	17.09	-11.55	5.54
	1500	27.38	-17.84	9.54
4	0300	35.49	-18.60	16.89
	1500	38.80	-15.63	23.17
5	0300	40.75	-14.45	26.30
	1500	43.73	-14.14	29.59
6	0300	45.43	-11.88	33.55
	1500	44.89	-9.89	35.00
7	0300	45.29	-10.26	35.03
	1500	45.11	-8.11	37.00

Table 5. Continued

Date	Time (GCT)	(ϕv_{ng})	(ϕv_{na})	(ϕv_{n})
8 February	0300	40.59	-1.26	39.43
	1500	34.90	3.92	38.82
9	0300	29.26	5.19	34.45
	1500	25.67	3.52	29.19
10	0300	27.22	0.77	27.99
	1500	29.76	2.16	31.92
11	0300	30.09	5.61	35.70
	1500	28.15	6.95	35.10
12	0300	23.73	8.38	32.11
	1500	20.49	10.95	31.44
13	0300	18.89	14.46	33.35
	1500	17.72	15.99	33.71
14	0300	17.85	14.43	32.28
	1500	18.07	11.88	29.95

It is evident from these values that the (ϕv_n) term computed with geostrophic winds alone, could be very much in error. Further, since the magnitude of this term is largely dependent on ϕ, any errors in v_n due to the geostrophic assumption would be magnified and could lead to spurious dissipation rate estimates in the final energy balance. So far as can be ascertained, no previous attempts at evaluating this term for a limited volume have been made. On the other hand, in previous investigations (Jensen, 1960; Barnes, 1962) of the kinetic energy budget of the stratosphere over the Northern Hemisphere, either this term was neglected or only a partial evaluation of its magnitude at the equator was carried out.

The rates of change of kinetic energy in the volume during the four sub-periods due to the (ϕv_n) process are shown in Table 6.

Table 6. Average values of (ϕv_n), in units of 10^{24} ergs per hour.

Period	(ϕv_n)
17 January to 25 January	-5.91
25 January to 4 February	-14.77
4 February to 9 February	116.86
9 February to 14 February	116.55

Generation of kinetic energy at the boundary pressure surfaces

The rates of change of kinetic energy in the volume as well as in the 100-50 mb and 50-25 mb layers due to the $(\phi\omega)$ process were computed according to the finite difference summation procedure shown in equation (20). The results of the computations are shown in Table 7.

Table 7. Rate of change of kinetic energy of the volume due to the $(\phi\omega)$ process, in units of 10^{21} ergs per second.

Date	Time (GCT)	$(\phi\omega)$ 100-50 mb	$(\phi\omega)$ 50-25 mb	$(\phi\omega)$ Volume
17 January	0300	-2.14	5.57	3.44
	1500	0.87	4.48	5.35
18	0300	1.10	3.49	4.59
	1500	-1.88	3.38	1.51
19	0300	-5.16	4.08	1.08
	1500	-3.36	4.95	1.58
20	0300	-0.19	4.31	4.12
	1500	-2.82	4.05	1.23
21	0300	-3.02	5.11	2.09
	1500	3.51	4.18	7.68
22	0300	5.90	2.48	8.38
	1500	7.68	2.83	10.51

Table 7. Continued

Date	Time (GCT)	$(\phi\omega)$ 100-50 mb	$(\phi\omega)$ 50-25 mb	$(\phi\omega)$ Volume
23 January	0300	1.09	3.[illegible]5	14.11
	1500	1.12	3[illegible]8	14.86
24	0300	8.72	4.[illegible]3	13.45
	1500	3.98	4.[illegible]4	8.22
25	0300	3.30	4.0[illegible]5	7.35
	1500	7.17	4.9[illegible]4	12.11
26	0300	10.62	4.9[illegible]5	15.57
	1500	13.43	4.0[illegible]2	17.45
27	0300	12.55	4.9[illegible]	17.52
	1500	11.88	7.5[illegible]	19.47
28	0300	15.65	7.74	23.40
	1500	17.67	7.03	24.71
29	0300	13.93	9.12	23.05
	1500	8.73	12.56	21.29
30	0300	5.89	13.54	19.43
	1500	7.35	11.97	19.33
31	0300	12.03	11.01	23.04
	1500	15.38	9.53	24.90
1 February	0300	18.53	7.57	26.10
	1500	17.16	7.79	24.96
2	0300	17.28	6.77	24.05
	1500	8.78	2.63	11.41
3	0300	10.76	0.81	11.57
	1500	8.36	2.47	10.83
4	0300	1.98	2.01	3.99
	1500	-1.50	-1.22	-2.72
5	0300	-0.64	-4.61	-5.25
	1500	-1.36	-6.99	-8.35
6	0300	-3.60	-7.49	-11.10
	1500	-3.44	-8.87	-12.31
7	0300	-1.71	-12.52	-14.23
	1500	-1.95	-15.90	-17.85
8	0300	-1.16	-17.63	-18.79
	1500	-1.91	-18.86	-20.77
9	0300	-5.30	-13.27	-18.58
	1500	-0.99	-14.44	-15.43
10	0300	-0.95	-11.43	-12.38
	1500	-7.03	-11.98	-19.01
11	0300	-11.04	-13.22	-24.26
	1500	-11.60	-11.95	-23.54
12	0300	-9.79	-10.31	-20.09
	1500	-9.24	-10.67	-19.91
13	0300	-14.02	-10.42	-24.44
	1500	-16.65	-8.47	-25.12
14	0300	-14.37	-8.20	-22.58
	1500	-12.38	-10.61	-22.99

The most striking feature of these results is the occurrence of consistently positive values for the volume from the beginning of the period until about 4 February and consistently negative values thereafter. In terms of rate of change of kinetic energy in the volume, this implied that the volume gained kinetic energy during the period 17 January to 4 February and lost kinetic energy after 4 February, through net generation at the upper and lower boundary surfaces. It is also of interest to note that, except in the beginning of the period, the volume always gained kinetic energy through generation at the 25-mb surface and lost kinetic energy through dissipation at the 100-mb surface. This can be seen from Fig. 10 in which the values of $\Sigma (Z\omega)_i \Delta A_i$, at each level, are plotted for each map time.

On the first two days, the generation process, mathematically equivalent to the vertical transfer of potential energy, showed upward transfer through the three pressure surfaces. This implied gain of kinetic energy by generation through net upward motion at 100 mb and loss by dissipation through net upward motion at 25 mb. The gain was greater than the loss, so that the $(\phi\omega)$ term was positive.

From 19 January until the end of the period, the values of $\Sigma (Z\omega)_i \Delta A_i$ at each level were consistently positive, implying a downward transfer of potential energy. During the period 19 January to 4 February, the gain of kinetic energy due to generation through net downward motion at 25 mb exceeded the loss due to dissipation through net downward motion at 100 mb. After 4 February, the loss through dissipation at 100 mb exceeded the gain through generation at 25 mb.

The rate of generation of kinetic energy in the 50-25 mb layer

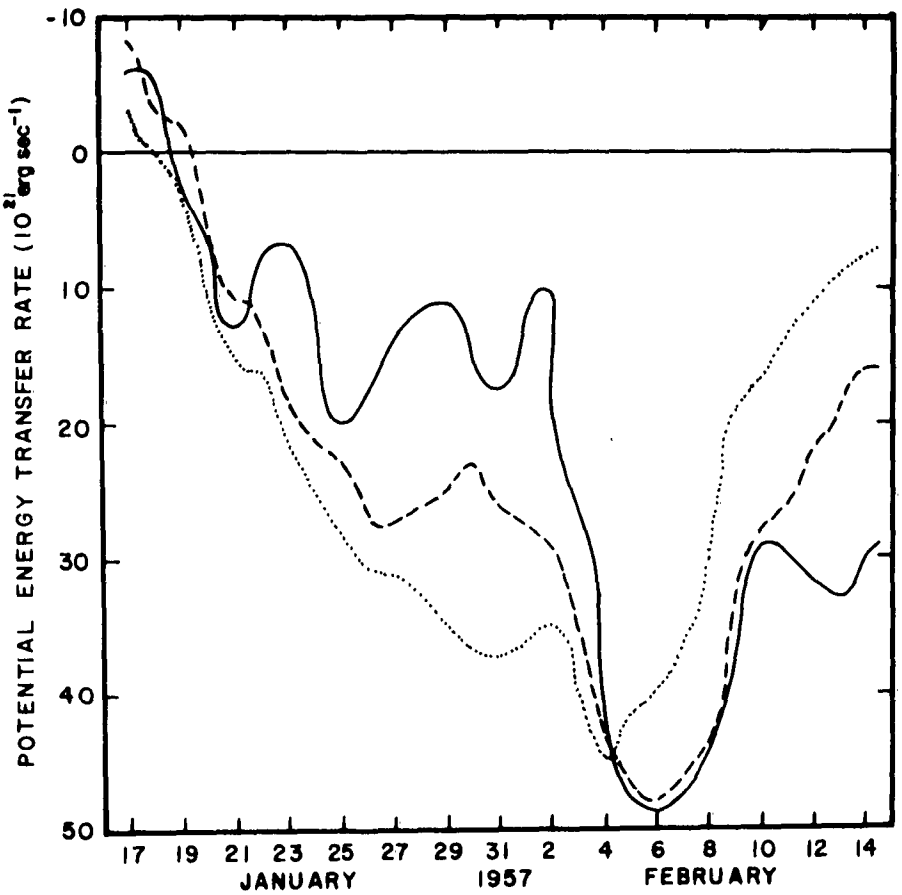

Fig. 10. Vertical transfer rate of potential energy through the 100-mb (solid line) 50-mb (dashed line) and 25-mb (dotted line) surfaces. Positive values denote downward transfer of energy.

was positive before 4 February and negative thereafter. The ($\phi\omega$) process in the 100-50 mb layer maintained the same sign as in the higher layer from about 21 January till the rest of the period. The reversal in sign that occurred on 4 February was simultaneous in both the layers.

The rates of change of kinetic energy in the volume during the four subperiods due to the ($\phi\omega$) process, are shown in Table 8.

Table 8. Average values of ($\phi\omega$), in units of 10^{24} ergs per hour.

Period	($\phi\omega$)
17 January to 25 January	24.86
25 January to 4 February	67.74
4 February to 9 February	-38.67
9 February to 14 February	-73.82

Correspondence between variations in the ($\phi\omega$) process and the ω patterns

It is of interest to view the variations in both magnitude and sign of the ($\phi\omega$) process as related to the radical changes that occurred in the ω fields at the three levels during the course of the warming.

Except during the first few days, the positive rate of generation of kinetic energy in the volume as well as in the two layers before 4 February, was brought about by a larger generation rate or synonymously speaking, a larger downward transfer of potential energy through the upper boundary (25 mb) surface as compared to the downward transfer through the lower boundary surface (100 mb). The ω maps for 25 January indicate that the large-scale downward motion at 25 mb, contributed to

such a large downward transfer at this level. The occurrence of large scale downward motion at 25 mb from 23 January to about 2 February with no marked changes in the ω patterns at the lower levels, was associated with the positive values of the ($\phi\omega$) term or relatively high rates of generation of kinetic energy during this period.

After 2 February, radical changes took place at the 50-mb and 100-mb levels. As described in Section 5, there was a tendency for downward motion at these levels to occupy increasingly larger areas (Fig. 4). Associated with this, the downward transfer of energy through the 100-mb surface began to increase in magnitude. By about 4 February, the downward transfer through 100 mb exceeded that through the higher levels, resulting in large negative values of the ($\phi\omega$) term or dissipation of kinetic energy in the volume.

The changes in the ω fields and the associated variations in magnitude and sign of the energy generation rate in the volume through generation at the boundaries, can be briefly summarized as follows. Generation of kinetic energy at the 25-mb surface in association with a general sinking motion at this level acted to increase the kinetic energy of the underlying atmospheric volume. The establishment of large scale sinking motion at the lower pressure levels acted to decrease the kinetic energy of the overlying layers through dissipation at the lower boundary surfaces.

The combined generation rate due to the (ϕv_n) and ($\phi\omega$) processes

For convenient reference, the values of the (ϕv_n) and ($\phi\omega$) terms and the total generation rate they represented, are given below.

Table 9. Average values of $(\phi v_n)+(\phi\omega)$, in units of 10^{24} ergs per hour.

Period	(ϕv_n)	$(\phi\omega)$	$(\phi v_n)+(\phi\omega)$
17 January to 25 January	-5.91	24.86	18.95
25 January to 4 February	-14.77	67.74	52.97
4 February to 9 February	116.86	-38.67	78.19
9 February to 14 February	116.55	-73.82	42.73

As in the case of the advection processes described in Section 7, the (ϕv_n) and $(\phi\omega)$ processes also acted in opposite sense or, partially compensated each other to give a net positive kinetic energy generation rate for the volume. In terms of the dynamics of the processes, the loss of kinetic energy through dissipation at the vertical boundaries and at the 100-mb surface, was compensated by a gain through generation at the 25-mb surface. Later, a gain in kinetic energy through generation at the vertical boundaries and at the 25-mb surface, was reduced by dissipation at the 100-mb surface. If we view the processes as equivalent to flux of potential energy, horizontal divergence or convergence of the potential energy flux produced a corresponding vertical convergence or divergence of the flux through the constant pressure surfaces.

Order of magnitude of the generation rates

The values obtained for the (ϕv_n) and $(\phi\omega)$ processes are an order of magnitude larger than the corresponding values for (kv_n) and $(k\omega)$ processes discussed in the previous section. This is in agreement with what one would expect by a scale factor analysis. Denoting scale

equivalence by the symbol [ ], we may write $V = \frac{1}{f}\frac{\partial \phi}{\partial n} = \left[\frac{\phi}{fL}\right]$, where V is the wind velocity and L is a characteristic length.

The ratio $\frac{\text{kinetic energy}}{\text{potential energy}}$ varies as

$$\frac{V^2}{\phi} = \left[\frac{1}{f} \cdot \frac{\phi}{f L^2}\right] \tag{34}$$

Relative vorticity

$$\zeta = \left[\frac{V}{L}\right] = \left[\frac{\phi}{f L^2}\right] \tag{35}$$

Thus,
$$\frac{V^2}{\phi} = [\zeta/f] \doteq \left[\frac{10^{-5}}{10^{-4}}\right] = [1/10] \tag{36}$$

As mentioned in Section 7, the (kv_n) term representing horizontal flux of kinetic energy was evaluated using the geostrophic u and v components across the perimeter increments. In view of the near geostrophic equilibrium observed at stratospheric levels and the fact that the (kv_{ng}) term was relatively unimportant in the kinetic energy balance, the evaluation of (kv_{na}) term was not considered essential. But the inclusion of the (ϕv_{na}) process in the evaluation of the (ϕv_n) term, was necessary in order to obtain a closer estimate of the actual horizontal flux of potential energy. It is easily seen that the integral of ϕv_{ng} around the closed perimeter L would be zero but for the variations of f along L. The (ϕv_{na}) term, however, depended heavily on the magnitudes of ϕ. Any errors in v_n due to the ageostrophic component, would, therefore be greatly magnified in the summation of the products of ϕ and v_{na} and could lead to spurious values for the (ϕv_n) term.

9. GENERATION OF KINETIC ENERGY WITHIN THE VOLUME BY CONVERSION FROM POTENTIAL ENERGY

The rate of conversion of available potential energy into the kinetic energy of the horizontal wind is given by the (ωT) term of equation (12). The finite difference approximation used for the evaluation of this term is shown in equation (21). That this term actually represents a conversion of potential and internal energy to kinetic energy has been demostrated by previous investigators (e.g., White and Saltzman, 1956). The physical mechanism for such conversion is the sinking of cold air mass, and the rising of warm air mass. In what follows, any statement about conversion of potential energy implies conversion of the sum of potential and internal energy of the volume.

The rates of generation of kinetic energy in the volume due to the conversion process, (ωT), are given in Table 10. Except in the beginning of the period, this process consistently represented dissipation of kinetic energy in the volume through conversion to potential energy. The values for the conversion term within the 100-50 mb and 50-25 mb layers treated separately, are plotted in Fig. 11. During the first two days of the period, kinetic energy in both the layers was increasing due to conversion from potential energy. From 19 January to about 24 January, the kinetic energy dissipation rate due to a reverse transformation from kinetic to potential energy was, in general, of the same magnitude in both the layers. The dissipation rate due to the conversion process was higher in the 50-25 mb layer than in the 100-50 mb

layer between 25 January and about 3 February and vice versa thereafter until the end of the analysis period. The rapidity of the warming at 25 mb from 24 January to 3 February corresponded to the consistent high values of the (ωT) term during this period. The occurrence, later on, of large scale descent and rapid temperature increases at the lower levels corresponded to the group of maximum values of the (ωT) term from about 4 February to 9 February.

Table 10. Rate of change of kinetic energy of the volume due to conversion from potential energy, in units of 10^{21} ergs per second.

Date	Time (GCT)	(ωT)
17 January	0300	2.87
	1500	2.07
18	0300	1.33
	1500	0.93
19	0300	0.05
	1500	-1.22
20	0300	-3.24
	1500	-5.21
21	0300	-5.61
	1500	-5.47
22	0300	-5.93
	1500	-6.55
23	0300	-7.53
	1500	-8.37
24	0300	-8.97
	1500	-10.34
25	0300	-11.20
	1500	-11.26
26	0300	-11.68
	1500	-11.92
27	0300	-11.85
	1500	-11.76
28	0300	-11.44
	1500	-11.26
29	0300	-11.52
	1500	-11.79
30	0300	-12.17
	1500	-12.57

Table 10. Continued

Date	Time (GCT)	(ωT)
31 January	0300	-12.50
	1500	-12.78
1 February	0300	-12.94
	1500	-12.59
2	0300	-13.47
	1500	-14.98
3	0300	-16.09
	1500	-18.06
4	0300	-20.51
	1500	-21.23
5	0300	-21.05
	1500	-21.87
6	0300	-22.41
	1500	-21.77
7	0300	-21.49
	1500	-21.48
8	0300	-20.04
	1500	-17.77
9	0300	-15.58
	1500	-13.31
10	0300	-12.04
	1500	-11.88
11	0300	-11.54
	1500	-10.96
12	0300	-9.96
	1500	-9.06
13	0300	-8.86
	1500	-8.31
14	0300	-7.59
	1500	-7.57

The values of the rate of dissipation of kinetic energy within the volume through conversion to potential energy, during the four sub-periods are shown in Table 11.

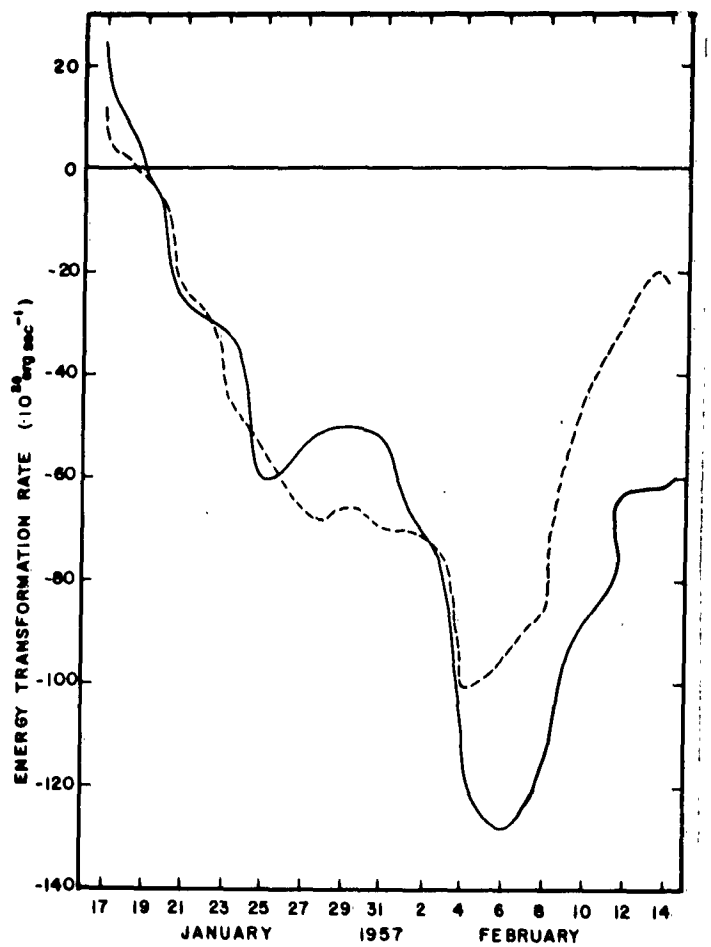

Fig. 11. Rate of conversion of kinetic to potential energy within the 100-50 mb layer (solid line) and within the 50-25 mb layer (dashed line). Negative values indicate conversion from kinetic to potential energy.

Table 11. Average values of (ωT), in units of 10^{24} ergs per hour.

Period	(ωT)
17 January to 25 January	-16.55
25 January to 4 February	-46.53
4 February to 9 February	-74.57
9 February to 14 February	-37.66

In view of the limited volume chosen for the present study, no attempt was made to evaluate the total conversion rates in terms of conversions due to either zonal eddies and meridional overturnings or in terms of conversions in different wave numbers. The conversion rates obtained for the lower stratospheric layer over the north American continent should, however, be viewed in relation to the conversion between available potential energy and total kinetic energy over the rest of the Northern Hemisphere. In this connection, the estimates of conversion rates of zonal and eddy available potential energy, made by Wolfe (1960) and Reed (1962) are of particular interest. These estimates were made for the period 25 January to 9 February, 1957 which is only a part of the time period used in this study. But the area chosen by them covered the Northern Hemisphere between latitudes 30N and 85N. The values obtained by them both for zonal conversions and eddy conversions at the 50-mb level are two orders of magnitude smaller than the average conversion rates computed for the 100-50 mb layer over North America, for the same period. In view of the differing methods of averaging used,

especially in the computation of vertical motions, the two sets of values are not strictly comparable. Also, the area over which the intense warming occurred was only a small portion of the Northern Hemisphere. The extremely large values for the conversion rates over the analysis area as compared to those on a hemispheric scale would, therefore, indicate that the rapid conversion to potential energy in the area of the stratospheric warming was a major sink for the hemispheric kinetic energy.

Net generation of kinetic energy in the volume

The values for the rate of change of kinetic energy due to the generation processes (ϕv_n) and $(\phi\omega)$ at the boundaries of the volume and the conversion process (ωT) within the volume, are presented in Table 12, for immediate reference and comparison purposes.

Table 12. Average values of the net generation rate, in units of 10^{24} ergs per hour.

Period	$(\phi v_n)+(\phi\omega)$	(ωT)	Net generation rate
17 January to 25 January	18.95	-16.55	2.40
25 January to 4 February	52.97	-46.53	6.44
4 February to 9 February	78.19	-74.57	3.62
9 February to 14 February	42.73	-37.66	5.07

10. ENERGY TRANSPORT AND GENERATION PROCESSES IN TERMS OF MEAN AND EDDY CONTRIBUTIONS

In many previous investigations of the energy transport and transformation processes based on hemispheric data (e.g., Jensen, 1960) the usual procedure was to divide the terms representing these processes into their mean values and deviations from the mean values. The latter were again subdivided to yield the contributions from vertical motions in a zonal plane, meridional overturnings and synoptic scale vertical motions associated with migratory cyclones and anticyclones. Although a closed pressure surface around the earth was not used, it was customary to neglect the mean values of the terms which were due to mean vertical motions over the portion of the hemisphere actually used in the analysis. Over an area much larger than the scale of the vertical motions, one would normally expect their mean value to be nearly zero, areas of downward and upward motion cancelling each other. But the limited extent of the analysis area and depth of stratospheric layer used in the present study, precluded any such analysis based on zero mean vertical motion. The mean ω over the analysis area was, in fact, consistently positive during most of the period and the contribution of the mean motion to the values of $(k\omega)$, $(\phi\omega)$ and (ωT) terms could be quite significant.

Since the dominant scale of motion during the warming was wave number two, it must be emphasized here, that the mean motion over the analysis area would only correspond to what may be termed a large scale

eddy motion on a hemispheric scale. In what follows, therefore, the mean motion and the eddies which involve departures from the mean motion refer only to the limited portion of the dominant planetary wave covered by the analysis area.

The procedure adopted for the treatment of the ($k\omega$), ($\phi\omega$) and (ωT) processes in terms of mean motion and eddies was based on the classification scheme proposed by Benton and LaSeur (1953). Following the nomenclature used by them, the residual flow that remained after the mean motion was subtracted out of the total flow, consisted of space eddies, time eddies and space-time eddies. The space eddies were defined as "eddies which remain after averaging over the time period under consideration." Such eddies would, therefore, show up on time-mean charts. The fluctuations in intensity of these space eddies were attributed to other eddies. Time eddies were defined as "eddies which appear in time after averaging over the entire space field under consideration." The time eddies would reveal any periodicities in the variations of the total flow pattern during the particular time period. Space-time eddies were defined as "eddies which disappear when the motion is averaged either over the space field or the time field under consideration." The migratory cyclones and anticyclones of middle latitudes are examples of space-time eddies.

For the purposes of the present study, "space" denoted the area in Fig. 1 and the time periods used were the four subperiods mentioned previously. Accordingly, the expression for the contributions to the vertical transport of kinetic energy due to the mean motion and the various eddies of a two-dimensional flow can be written as follows.

$$\left(k_{ii}\omega_{ii}\right)_{st} = k_{st}\omega_{st} + \left(k_{si}\omega_{si} - k_{st}\omega_{st}\right)_{t} + \left(k_{it}\omega_{it} - k_{st}\omega_{st}\right)_{s} +$$

$$\left(k_{ii}\omega_{ii} - k_{si}\omega_{si} - k_{it}\omega_{it} + k_{st}\omega_{st}\right)_{st} \qquad (37)$$

where,

s denotes averaging over area

t denotes averaging over time

st denotes averaging over area and time

ii denotes the value at the i^{th} grid point at t = i

si denotes the areal mean value at t = i

it denotes the time mean value at the i^{th} grid point

$k_{ii}\omega_{ii}{}_{st}$ is the time average of the vertical transport term, $\frac{1}{g}\Sigma\ k\omega_{i}\ \Delta A_i$, through any pressure level.

The first and second terms on the right side of (37) represent the average vertical transport of kinetic energy through any pressure surface due to the mean motion and time eddies respectively. The third and fourth terms give the contributions due to space eddies and space-time eddies. In view of the large scale and slow changes and movement of systems in the stratosphere, it was decided to group these two terms together under the name "space eddies."

The actual evaluation of the terms in (37) for each pressure level and during each of the four subperiods was done as follows.

$$\left(k_{ii}\omega_{ii}\right)_{st} \doteq \frac{1}{NA}\left[\left(\Sigma(k\omega)_i\ \Delta A_i\right)_{t=1}(6\text{ hrs}) + \left(\Sigma(k\omega)_i\ \Delta A_i\right)_{t=2}(12\text{ hrs}) + \right.$$

$$\left. \ldots + \left(\Sigma(k\omega)_i\ \Delta A_i\right)_{t=n-1}(12\text{ hrs}) + \left(\Sigma(k\omega)_i\ \Delta A_i\right)_{t=n}(6\text{ hrs})\right] \qquad (38)$$

where, N = number of hours during the subperiod and n is the number of maps during the subperiod. For example, for the period 0300 GCT, 17 January to 0300 GCT, 25 January, t = 1 meant map for 0300 GCT of 17 January, t = 2 meant map for 1500 GCT of 17 January and t = n meant map for 0300 GCT of 25 January.

$$\omega_{st} \doteq \frac{1}{NA}\left[\left(\Sigma\omega_i\ \Delta A_i\right)_{t=1}(6\text{ hrs}) + \left(\Sigma\omega_i\ \Delta A_i\right)_{t=2}(12\text{ hrs}) + \ldots\right.$$

$$\left. \ldots + \left(\Sigma\omega_i\ \Delta A_i\right)_{t=n-1}(12\text{ hrs}) + \left(\Sigma\omega_i\ \Delta A_i\right)_{t=n}(6\text{ hrs})\right] \qquad (39)$$

Similar expressions could be written down for k_{st}, ϕ_{st} and T_{st}.

Substitution of ϕ or T for k in (38) yielded expressions for $(\phi\omega)_{st}$ and $(\omega T)_{st}$ for each pressure level.

$$\left(k_{si}\omega_{si} - k_{st}\omega_{st}\right)_t \doteq \frac{1}{N}\left[\left(\frac{\Sigma k_i\ \Delta A_i}{A}\right)_{t=1}\left(\frac{\Sigma\omega_i\ \Delta A_i}{A}\right)_{t=1}(6\text{ hrs}) + \right.$$

$$\left(\frac{\Sigma k_i\ \Delta A_i}{A}\right)_{t=2}\left(\frac{\Sigma\omega_i\ \Delta A_i}{A}\right)_{t=2}(12\text{ hrs}) + \ldots + \left(\frac{\Sigma k_i\ \Delta A_i}{A}\right)_{t=n}$$

$$\left.\left(\frac{\Sigma\omega_i\ \Delta A_i}{A}\right)_{t=n}(6\text{ hrs})\right] - k_{st}\omega_{st} \qquad (40)$$

The evaluation of the space eddy term given by the sum of the third and fourth terms was not done directly but obtained as a residual out of the imbalance among the other terms.

Vertical integration of expressions (38), (39), (40) and similar expressions involving ϕ and T, gave the contributions to the particular processes in the layer through which the integration was carried out.

The (kω) process - mean and eddy contributions

The values for the mean term, $k_{st}\omega_{st}$ and the space and time eddy terms at the three pressure levels as well as their contributions to the vertical transport of kinetic energy through the layers, are given in Tables 13 and 14 respectively.

The most obvious feature of these results is the relative importance of the vertical transport of kinetic energy through mean sinking motion at the upper and lower boundary surfaces of the layers.

Almost the entire period of analysis was characterized by a net downward transport of kinetic energy at the three pressure levels. As indicated in Section 7, the positive contribution to kinetic energy increase in the layers as well as in the volume, during the first two subperiods was, in general, due to a larger downward transport rate through 25 mb and successively lower rates through the 50 and 100-mb levels. The negative values from 4 February to 14 February were due to a larger downward transport through 100 mb and successively less downward transport through the higher levels. The values of ω at each level, when averaged over the area, were also positive, except for two days in the beginning of the analysis period.

As in the case of transport of kinetic energy through mean downward motion, the transports at all levels through space eddies represented by the covariance of k and ω over the analysis area, were consistently downward at each pressure level. The positive contribution from these eddies for the period 17 January to 25 January was due to a larger downward transport through the upper boundary of the layer than through the lower boundary. The negative contributions arose from

Table 13. Vertical transport of kinetic energy, in units of 10^2 ergs cm^{-2} sec^{-1} through the pressure levels due to the mean motion and the eddy components. Positive value indicates downward transport of energy.

Period	Level	Mean motion	Space eddy	Time eddy
17 January to 25 January	25 mb	1.34	0.77	-0.02
	50 mb	1.07	0.50	0.06
	100 mb	0.93	0.13	0.03
25 January to 4 February	25 mb	4.38	1.12	-0.01
	50 mb	3.45	1.68	-0.08
	100 mb	2.77	1.90	0.00
4 February to 9 February	25 mb	2.40	1.79	0.13
	50 mb	4.21	3.30	0.03
	100 mb	6.09	4.66	0.03
9 February to 14 February	25 mb	0.28	0.11	0.03
	50 mb	1.09	0.61	0.04
	100 mb	2.81	1.38	0.01

Table 14. Contributions to the ($k\omega$) process, in units of erg cm^{-2} mb^{-1} sec^{-1} due to mean motion and eddy components. Positive value indicates contribution acted to increase horizontal kinetic energy.

Period	Layer	Mean motion	Space eddy	Time eddy
17 January to 25 January	50-25 mb	1.07	1.08	-0.31
	100-50 mb	0.30	0.75	0.07
	100-25 mb	0.50	0.84	-0.05
25 January to 4 February	50-25 mb	3.73	-2.22	0.28
	100-50 mb	1.37	-0.44	-0.15
	100-25 mb	1.94	-0.93	-0.01
4 February to 9 February	50-25 mb	-7.26	-6.02	0.40
	100-50 mb	-3.76	-2.73	-0.01
	100-25 mb	-4.43	-3.44	0.11
9 February to 14 February	50-25 mb	-3.26	-2.01	-0.03
	100-50 mb	-3.44	-1.54	0.06
	100-25 mb	-3.04	-1.53	0.04

reversed conditions at the upper and lower boundary pressure surfaces. The consistently positive values of the covariance of k and ω at each level, also indicated a preference for downward motion to occur in areas of high wind speeds, at least over the portion of the long wave pattern covered by the analysis area.

The relative unimportance of the time eddies serves to illustrate the slow changes in stratospheric systems.

The $(\phi\omega)$ process - mean and eddy contributions

The values for the mean term $\phi_{st}\omega_{st}$ as well as for the space and time eddies at each pressure level are given in Table 15. The contributions to the $(\phi\omega)$ process in the layers are shown in Table 16.

The magnitudes of the mean motion terms show that large scale downward motion over the analysis area during the warming period accounted for almost all of the generation process $(\phi\omega)$.

The magnitudes of the contribution from space eddies were very small in comparison with those due to mean sinking motion.

An interesting aspect of the space eddies is the reversal in sign to that of the mean motion term in certain layers and in some of the subperiods. Values of the space eddy terms at each pressure level (Table 15) showed that these terms were negative at all levels that is, transferred energy upwards, or increased kinetic energy of the overlying layers, from 17 January to 4 February. During 4 February to 9 February, they were positive only at 100 mb and after 9 February at 25 and 50 mb. The predominantly negative values of the space eddy terms at all levels would indicate that downward motion was in general associated with low values of ϕ, that is, with troughs and upward motion with ridges.

reversed conditions at the upper and lower boundary pressure surfaces. The consistently positive values of the covariance of k and ω at each level, also indicated a preference for downward motion to occur in areas of high wind speeds, at least over the portion of the long wave pattern covered by the analysis area.

The relative unimportance of the time eddies serves to illustrate the slow changes in stratospheric systems.

The $(\phi\omega)$ process - mean and eddy contributions

The values for the mean term $\phi_{st}\omega_{st}$ as well as for the space and time eddies at each pressure level are given in Table 15. The contributions to the $(\phi\omega)$ process in the layers are shown in Table 16.

The magnitudes of the mean motion terms show that large scale downward motion over the analysis area during the warming period accounted for almost all of the generation process $(\phi\omega)$.

The magnitudes of the contribution from space eddies were very small in comparison with those due to mean sinking motion.

An interesting aspect of the space eddies is the reversal in sign to that of the mean motion term in certain layers and in some of the subperiods. Values of the space eddy terms at each pressure level (Table 15) showed that these terms were negative at all levels that is, transferred energy upwards, or increased kinetic energy of the overlying layers, from 17 January to 4 February. During 4 February to 9 February, they were positive only at 100 mb and after 9 February at 25 and 50 mb. The predominantly negative values of the space eddy terms at all levels would indicate that downward motion was in general associated with low values of ϕ, that is, with troughs and upward motion with ridges.

Table 15. Vertical transfer of potential energy, in units of 10^2 ergs cm^{-2} sec^{-1} through the pressure surfaces due to the mean motion and the eddy components. Positive value indicates downward transfer of energy.

Period	Level	Mean motion	Space eddy	Time eddy
17 January to 25 January	25 mb	463.70	-6.22	1.59
	50 mb	319.62	-3.83	-1.28
	100 mb	235.77	-5.67	-0.68
25 January to 4 February	25 mb	1262.90	-3.70	0.50
	50 mb	1010.40	-5.30	0.30
	100 mb	616.49	-11.32	0.22
4 February to 9 February	25 mb	1297.20	-3.90	-1.30
	50 mb	1668.70	-1.40	-0.09
	100 mb	1691.30	2.20	0.03
9 February to 14 February	25 mb	435.60	0.40	0.20
	50 mb	841.60	1.20	0.00
	100 mb	1163.70	-3.80	-0.06

Table 16. Contributions to the ($\phi\omega$) process, in units of erg cm^{-2} mb^{-1} sec^{-1} due to mean motion and eddy components. Positive value indicates contribution acted to increase horizontal kinetic energy.

Period	Layer	Mean motion	Space eddy	Time eddy
17 January to 25 January	50-25 mb	576.3	-9.6	11.2
	100-50 mb	167.7	3.7	-1.2
	100-25 mb	296.3	-0.7	2.9
25 January to 4 February	50-25 mb	1010.0	6.4	0.8
	100-50 mb	787.3	12.0	0.2
	100-25 mb	840.3	9.9	0.4
4 February to 9 February	50-25 mb	-1486.0	-10.0	-4.8
	100-50 mb	-45.2	-7.2	-0.2
	100-25 mb	-512.3	-7.9	-1.7
9 February to 14 February	50-25 mb	-1624.0	-3.2	0.8
	100-50 mb	-644.0	10.0	0.1
	100-25 mb	-946.5	5.5	0.3

Jensen (1960) has noted the same type of relationship in certain eddies in the 100-50 mb layer.

It was pointed out in Section 8 that the ($\phi\omega$) process, except in the beginning of the period, was characterized by a gain of kinetic energy for the layers through generation at the upper boundary surfaces and a loss due to dissipation at the lower boundary surfaces. The same argument applied to the mean motion contribution to the ($\phi\omega$) process. But this was not the case, in general, with space eddies. The covariance of ϕ and ω were such that, more often the layers lost kinetic energy owing to dissipation through eddy vertical motions at the boundary surfaces.

As in the case of the ($k\omega$) process, the contributions due to the time eddies were very small.

The (ωT) process - mean and eddy contributions

The magnitudes of the conversion processes within the layers due to mean sinking motions over the analysis area and due to the eddies are shown in Table 17.

Compared to the contributions to the conversion process from the mean sinking motions, those from the eddies were very small. The consistently large negative values of the conversion process due to large scale sinking motion over the analysis area would also imply the simultaneous existence of upward motion over other relatively cold areas on the hemisphere.

From the time when pronounced warming first began at 25 mb to the end of the analysis period, that is, from about 25 January onwards, the conversion processes due to the space eddies were also acting to

decrease kinetic energy. In the few days prior to the actual warming, that is, during the first subperiod, the conversions due to the space eddies were such that eddy potential energy was transformed to eddy kinetic energy. Since only a portion of the Northern Hemisphere is covered by the analysis area, it is not strictly possible to relate the conversion processes in the limited volume to zonal and eddy transformations on a hemispheric scale.

On the basis of the scales of motion involved, however, it would seem that the major portion of the kinetic to potential energy conversion occurred on a scale comparable to the analysis area. This is in agreement with the fact that the dominant scale of eddy motion during the warming was wave number two and the portion of the hemisphere under study was part of such a large scale eddy.

Table 17. Contributions to the (ωT) process, in units of erg cm^{-2} mb^{-1} sec^{-1} due to mean motion and eddy components. Positive value indicates contribution acted to increase horizontal kinetic energy

Period	Layer	Mean motion	Space eddy	Time eddy
17 January to 25 January	50-25 mb	-347.7	4.1	1.1
	100-50 mb	-144.9	1.5	0.8
	100-25 mb	-207.2	2.3	0.9
25 January to 4 February	50-25 mb	-980.6	-4.7	-1.1
	100-50 mb	-431.2	-5.9	0.0
	100-25 mb	-598.9	-5.3	-0.3
4 February to 9 February	50-25 mb	-1234.7	-14.6	1.1
	100-50 mb	-826.6	-14.9	0.0
	100-25 mb	-961.9	-14.5	0.3
9 February to 14 February	50-25 mb	-499.9	-1.2	-0.6
	100-50 mb	-496.4	-2.6	-0.2
	100-25 mb	-485.2	-2.1	-0.3

11. KINETIC ENERGY BUDGET OF THE VOLUME

The average values of the terms in equation (12) for the four time periods are listed in Table 18.

As mentioned previously, the terms involving transport of existing kinetic energy, namely the (kv_n) and $(k\omega)$ terms, are negligible in the kinetic energy budget of the volume. This is also confirmed by previous computations (Jensen, 1960; Barnes, 1962) covering the Northern Hemisphere.

Also, the time-change of kinetic energy in the volume turns out to be a very small quantity relative to some of the other terms. The time change of kinetic energy is usually neglected in most investigations on the basis that it does not change significantly over a period of time. In our case, there was a large change of kinetic energy in the volume in terms of the initial and final wind fields. However, from the point of view of the physical processes acting to change the kinetic energy in the volume, the actual change was of relatively small magnitude. Like many other meteorological quantities, the changes in kinetic energy are brought about by the small differences of other large terms.

During the first part of the period until 4 February, kinetic energy in the volume was generated through vertical motions at the upper boundary surface. It was dissipated through vertical motions at the lower boundary surface, through transfer to the surrounding atmosphere by the (ϕv_n) process as well as through conversion to potential energy.

During the latter part of the period, after 4 February, the $(\phi\omega)$

Table 18. Average values of terms in the kinetic energy balance equation, in units of 10^{24} ergs per hour. Positive value indicates process acted to increase kinetic energy of the volume.

	17 January-25 January	25 January-4 February	4 February-9 February	9 February-14 February
$\frac{\partial K}{\partial t}$	0.23	-0.09	-0.57	-0.19
(kv_n)	-0.57	-1.08	0.63	0.33
$(k\omega)_{25\ mb}$	0.22	0.55	0.43	0.04
$(k\omega)_{100\ mb}$	-0.10	-0.47	-1.07	-0.42
$(k\omega)$	0.12	0.08	-0.64	-0.38
(ϕv_n)	-5.91	-14.77	116.86	116.55
$(\phi\omega)_{25\ mb}$	47.67	125.72	128.85	43.60
$(\phi\omega)_{100\ mb}$	-22.81	-57.98	-167.52	-117.42
$(\phi\omega)$	24.86	67.74	-38.67	-73.82
$(\omega\Gamma)$	-16.55	-46.53	-74.57	-37.66
D	-1.72	-5.53	-4.18	-5.21

term was negative while the (ϕv_n) term became positive and large. The volume gained kinetic energy through the (ϕv_n) process and through generation at the upper boundary surface. It lost kinetic energy through dissipation at the lower boundary surface and through conversion to potential energy. The relatively high values of the (ϕv_n) term, also show that the magnitudes of the $(\phi\omega)$ and $(\omega\Gamma)$ terms may not be representative of the average stratosphere at all longitudes during this period.

The imbalance among the computed terms listed in Table 18, presumably represents D, the "frictional" dissipation of kinetic energy in the volume, by motions of smaller scale than are defined by the analysis. Estimates of D are also shown in Table 18. These estimates have been obtained as differences among three large terms and include to some extent, errors in the computations. Relative to the other processes in the volume, the magnitudes of the dissipation rates appear reasonable. In view of the fact that the volume covered only a limited portion of the Northern Hemisphere, these rates may not be representative of stratosperic motions on a hemispheric scale.

12. SUMMARY AND CONCLUSIONS

For the portion of the lower stratosphere over North America, bounded by the 100 and 25-mb pressure surfaces, the terms in the kinetic energy balance equation have been evaluated. Since the volume under study was an open system, energy exchanges with the surrounding atmosphere were taken into consideration. These exchanges took place not only between the adjacent layers above and below the volume but also along the vertical boundaries.

The actual variation of kinetic energy in the volume was found to result from a small difference among other large terms. As far as the kinetic energy budget of the volume was concerned, terms involving the vertical and horizontal transports of existing kinetic energy were shown to be negligible. This is in agreement with the results of previous investigations on the advection of kinetic energy on a hemispheric scale. Kinetic energy variations in the lower stratospheric layers should therefore be accounted for by consideration of other much larger generation processes. Such processes consist of conversion of potential to kinetic energy within the layers and generation of kinetic energy at the boundaries.

Previous investigators of energy conversions in stratospheric layers during other winters, have differed on the sign of the conversion process, (ωT). According to Starr (1959), the large hydrostatic stability present in the lower stratosphere indicates that this region is, on the average, one of forced vertical motions resulting in conversions of

kinetic to potential energy. Jensen (1960) found an overall positive transformation from potential to kinetic energy in the 200-50 mb layer, during January 1958, with a reverse transformation from kinetic to potential energy in the 100-50 mb layer. Barnes (1962) was of the view that the upper stratosphere above 40 mb was characterized by conversion from potential to kinetic energy. For the limited volume and time period used in this report, the conversion of energy within the volume as well as in the 100-50 mb and 50-25 mb layers, was generally in the direction from kinetic to potential energy.

Further work with data for long enough periods and at levels reaching 25 mb and above, is needed to ascertain the variations in magnitude and sign of the conversion process in the stratosphere. Previous investigators of energy transformations in stratospheric layers (Roberts, 1960; Hansrote and Lambert, 1960; Wolfe, 1960; Reed, 1962) have, however, agreed on the importance of boundary generation processes in the energy balance.

The (ϕv_n) and $(\phi\omega)$ terms for a limited volume or the $(\phi\omega)$ term in the case of a hemispheric layer with negligible interactions at the equator, represent processes generating kinetic energy through motions across the boundaries. For the entire atmosphere with zero vertical motions at the surface and at the top, the $(\phi\omega)$ term would, of course, vanish in the final summation of the integral representing this term. The importance of the $(\phi\omega)$ process in the kinetic energy budget of tropospheric layers, has been demonstrated by Jensen (1960). His evaluations for the 100-50 mb layer were, however, based on the assumption that the $(\phi\omega)$ term vanished over the 50-mb surface covering the

Northern Hemisphere.

For the volume and period under study, the ($\phi\omega$) process at the top and bottom boundaries were such that the volume gained kinetic energy owing to downward motions at the 25-mb surface and lost kinetic energy owing to downward motions at the 100-mb surface. Almost throughout the period, generation at the 25-mb pressure surface was an important and consistent source of kinetic energy while dissipation at the 100-mb surface, was an equally consistent sink of kinetic energy for the volume. The essential role of the ($\phi\omega$) process is further demonstrated by the fact that during the first part of the period, generation of kinetic energy at the 25-mb surface, was the only important source of kinetic energy in order to counteract the losses due to other processes. During the latter part of the period, the dissipation of kinetic energy at the 100-mb surface was an important sink in order to balance the large increase brought about by generation at the vertical boundaries.

The role of vertical motions at the upper boundaries of stratospheric layers, in the kinetic energy balance, is not usually recognized and is often neglected. It is unfortunate that the volume covered only a limited portion of the Northern Hemisphere. It is, therefore, difficult to assess the importance of the ($\phi\omega$) process in relation to conditions over the hemisphere. As pointed out in Section 8, the large scale of downward motions over North America was a significant contributory factor for the relatively large magnitude of the ($\phi\omega$) term, during the warming period. Teweles (1958) has described a simultaneous warming that took place over eastern Siberia with features at 100 mb very

similar to those of the North American warming. The possibility of another region over Siberia where substantial downward transfer of energy occurred at the stratospheric levels cannot, therefore, be excluded. Both the areas under the influence of the warming phenomena were situated north of latitude 50N. The covariance of ϕ and ω over the hemisphere south of this latitude could have been such that in the final summation over the hemisphere, the $(\phi\omega)$ process proved to be negligible. Recent computations of energy conversions over a major portion of the hemisphere (Reed, 1962) however, indicate that such was not the case. The lack of balance among the conversion processes was attributed to a "net vertical outflow of geopotential through the base of the stratosphere."

During the earlier part of the period, horizontal motions at the vertical boundaries resulted in a loss of kinetic energy for the volume while later on, such motions brought about an increase of kinetic energy. In other words, the (ϕv_n) term was a source of kinetic energy for the rest of the stratosphere during the period prior to the downward extension of pronounced warming to the lower levels. During the time when warming continued throughout the volume the (ϕv_n) term acted as a source of kinetic energy for the volume considered and a sink for the stratosphere. The transfer of energy from the volume to the surrounding stratosphere during the early stages of the warming is, perhaps, not unreasonable, because decrease of kinetic energy is associated with the warming phenomenon. What is surprising is the large generation of kinetic energy during the period of pronounced warming at the lower levels, due to horizontal transfer of energy from the

surrounding stratosphere.

The values of the dissipation rate due to small scale motions, appear reasonable in relation to the magnitudes of the various generation processes. These dissipation rates were obtained as differences among three large quantities and include to some extent, errors in the computations. The relative imporance of the (ϕv_n) term would also indicate that these dissipation rates might not be representative of the average stratospheric layer between 100 mb and 25 mb.

This study has been based on data for three pressure levels and over a limited area during a one month period. Evaluation of the results obtained over North America in terms of application on a hemispheric scale is, therefore, a difficult proposition. Moreover, the time period chosen for study is not necessarily a representative sample in time. Nevertheless, it is felt that the computational procedures adopted for the present investigation are fruitful. Because of the appreciable hydrostatic stability in the stratosphere, the unimportance of phase changes of water and slow time changes of temperature, computations of vertical motion by the adiabatic method should yield values of at least the right sign and order of magnitude. With the increasing availability of data reaching 25 mb and above, computations similar to those used here can be extended to cover larger areas over the hemisphere. When using longer periods of time, the systematic effects of long-term diabatic heating may be significant enough to be incorporated in vertical-motion computations.

The relative importance of the ($\phi\omega$) term shows that in the energy balance pertaining to layers of limited depth, the values of

this term both at the upper and lower boundaries should be considered. Inasmuch as vertical boundaries do exist for an atmospheric volume not covering the whole earth, the contribution to the kinetic energy generation due to the (ϕv_n) term must also be estimated in the absence of sufficient actual wind data on the boundaries. There is need for further studies similar to the current one, in order to supplement or modify the conclusions reached here.

REFERENCES

Barnes, A. A., 1962: The energy balance of the stratosphere during the I.G.Y. Ph. D. Thesis, M. I. T.

Benton, G. S., and N. E. LaSeur, 1953: The space time distribution of atmospheric eddies. Geophysical Research Paper No. 24, AFCRC Technical Report 53-55, 89-97.

Craig, R. A. and W. S. Hering, 1959: The stratospheric warming of January-February, 1957. J. Meteor., 16, 91-107.

Craig, R. A. and M. A. Lateef, 1961: The stratospheric warming over North America in 1957, III, Height, Temperature, Vorticity and Vertical Motion at the 25-mb Surface. Sci. Rpt. No. 3, AF 19 (604)-5471, The Florida State University, 17 pp.

Craig, R. A. and M. A. Lateef, 1962: Vertical Motion during the 1957 Stratospheric Warming. J. Geo. Res., 67. 1839-1854.

Craig, R. A., M. A. Lateef and R. A. Mitchem, 1961a: The Stratospheric Warming over North America in 1957, I, Height, Temperature, Vorticity and Vertical Motion at the 100-mb Surface. Sci. Rpt. No. 1, AF 19(604)-5471, The Florida State University, 22 pp.

_____, 1961b: The Stratospheric Warming over North America in 1957, II. Height, Temperature, Vorticity and Vertical Motion at the 50-mb Surface. Sci. Rpt. No. 2, AF 19(604)-5471, The Florida State University, 16 pp.

Hansrote, L. S. and J. K. Lambert, 1960: Energy Interactions between the troposphere and stratosphere. Masters Thesis, M. I. T.

Jensen, C. E., 1960: Energy transformations and vertical flux processes over the Northern Hemisphere. Sci. Rpt. No. 1, AF 19(604)-6108, M. I. T., 272 pp.

Muench, H. S., 1958: Analysis of synoptic charts in the stratosphere. Contributions to stratospheric meteorology, Geophysics Research Directorate Research Notes, No. 1, 1-9.

Palmén, E., 1960: On generation and frictional dissipation of kinetic energy in the atmosphere. Societas Scientiarum Fennica Commentationes Physico-Mathematicae, XXIV, 11 pp.

Reed, R. J., 1962: On the cause of the stratospheric sudden warming phenomenon. Paper presented at the Symposium on Stratospheric and Mesospheric Circulation, Berlin, Aug.

Roberts, D. L., 1960: Vertical transport of potential energy across isobaric surfaces. Masters Thesis, M. I. T.

Scherhag, R., 1952: Die explosionsartigen Stratosphärenwarmungen des Spätwinters 1951/1952. Berichte des Deutschen Wetterdienst in der U. S. Zone, No. 38, 51-63.

Shuman, F. G., 1957: Numerical methods in weather prediction, smoothing and filtering. Mon. Wea. Rev., 85, 357-361.

Starr, V. P., 1948: On the production of kinetic energy in the atmosphere. J. Meteor., 5, 193-196.

_____, 1959: Questions concerning the energy of stratospheric motions. Sci. Rpt. No. 1, AF 19(604)-5223, M. I. T., 12 pp.

Teweles, S., 1958: Anomalous warming of the stratosphere over North America in early 1957. Mon. Wea. Rev., 86, 377-396.

White, R. M. and G. F. Nolan, 1960: A Preliminary Study of the Potential to Kinetic Energy Conversion Process in the Stratosphere. Tellus, 12, 145-148.

White, R. M. and B. Saltzman, 1956: On conversions between potential and kinetic energy in the atmosphere. Tellus, 8, 357-363.

Wolfe, J. L., 1960: A harmonic analysis of the change of kinetic energy and the conversion of potential to kinetic energy in the lower stratosphere during a sudden warming period. Masters Thesis, Univ. of Washington.